J Clin Periodontol 2007; 34: 691–708 doi: 10.1111/j.1600-051X.2007.01097.x

Journal of Clinical Periodontology

Extracellular matrix expression and periodontal wound-healing dynamics following guided tissue regeneration therapy in canine furcation defects

Michael Christgau[1,2], Raul G. Caffesse[3], Gottfried Schmalz[1] and Rena N. D'Souza[4]

[1]Department of Operative Dentistry and Periodontology, University of Regensburg, Regensburg, Germany; [2]Private Practice, Düsseldorf, Germany; [3]Graduate Periodontics, Universidad Autonoma de Nuevo Leon, Monterrey, Mexico; [4]Department of Biomedical Sciences, Baylor College of Dentistry, Dallas, TX, USA

Christgau M, Caffesse RG, Schmalz G, D'Souza RN. Extracellular matrix expression and periodontal wound-healing dynamics following guided tissue regeneration therapy in canine furcation defects. J Clin Periodontol 2007; 34: 691–708. doi: 10.1111/j.1600-051X.2007.01097.x.

Abstract

Aim: Temporal and spatial expression pattern of extracellular matrix (ECM) components in furcation defects following guided tissue regeneration (GTR) compared with open-flap debridement (OFD).

Material and Methods: In 21 dogs, mandibular second and fourth pre-molars were treated with one non-resorbable and three different resorbable membranes. Third pre-molars were treated by OFD. After 2, 4, 8 weeks and 3, 6, and 12 months, tissues were analysed by immunohistochemistry for collagen I (Col-I) and III (Col-III), fibronectin (FN), bone sialoprotein (BSP), and osteopontin (OPN).

Results: At 2 weeks, the defect was mainly occupied by FN+ granulation tissue (GT), which was sequentially replaced by new connective tissue expressing FN, Col-I, and increasingly Col-III. Following superficial resorptions by OPN+ osteoclasts and odontoclasts, cementum and bone formation ensued with strong expression of BSP and OPN along bone and tooth surfaces. Deposition of Col-I, FN, BSP and OPN+ cementoid and osteoid became evident after 4 weeks. Extrinsic fibres of cementum and bone stained intensely for Col-III. The newly formed periodontal ligament expressed FN, Col-I, and Col-III, but no BSP or OPN.

Conclusions: The spatial ECM expression was similar for OFD and the different GTR methods, although the timing and quantity of ECM expression were influenced by wound stabilization and inflammatory reactions.

Key words: bone; bone sialoprotein; cementum; collagen; extracellular matrix; fibronectin; immunohistochemistry; osteopontin; periodontal ligament; periodontitis; regeneration

Accepted for publication 4 April 2007

Conflict of interest and source of funding statement

The authors declare that they have no conflict of interests. The study was partially supported by the German Research Association (Deutsche Forschungsgemeinschaft) Grant DFG Ch 192/1-1. Further support was provided by the Ethicon GmbH & Co KG, Norderstedt, Germany.

Periodontal disease is characterized by an irreversible destruction of the supporting tissues of a tooth, namely root cementum, alveolar bone, and periodontal ligament (PDL), caused by a host immune response to the bacterial infection (Reynolds & Meikle 1997). The complete regeneration of lost periodontal tissues is regarded as the ideal goal of periodontal therapy and still needs major attention in terms of research (Grzesik & Narayanan 2002, AAP Position Paper 2005, Zeichner-David 2006). Besides other attempts (Schwarz et al. 2006, Stratul et al. 2006), there are currently two general treatment strategies to achieve periodontal regeneration (AAP Position Paper 2005). The first involves the use of cell-occlusive barrier membranes for

© 2007 The Authors. Journal compilation © 2007 Blackwell Munksgaard

guided tissue regeneration (GTR) alone or in combination with different types of bone grafts (Tonetti et al. 2004, Stavropoulos & Karring 2005, Christgau et al. 2006b), and the second involves the application of biologically active mediators (e.g. enamel matrix derivative, morphogenetic proteins, or different polypeptide growth factors) (Giannobile & Somerman 2003, Christgau et al. 2006a). Several histological studies in animals (Karring et al. 1985, Caffesse et al. 1988, 1990, 1994, Pontoriero et al. 1992, Hammarström et al. 1997, Graziani et al. 2005, Laurell et al. 2006) and humans (Zappa 1991, Camelo et al. 1998, Sculean et al. 1999) as well as controlled clinical trials (Jepsen et al. 2002, Needleman et al. 2002, Trombelli et al. 2002, Murphy & Gunsolley 2003) have proven the potential of these methods to restore periodontal tissues partially. However, some essential drawbacks limit the therapeutic value of all the methods available so far. First, only a very narrow spectrum of space-making periodontal defects, i.e. deep intra-bony defects and mandibular class II furcation lesions, can be treated predictably (AAP Position Paper 2005). Supracrestal horizontal bone loss and class III furcation defects are not suitable for regenerative procedures. Second, the regeneration outcomes are characterized by a high variability and consequently low predictability. None of the mentioned methods has been proven to result consistently in complete periodontal regeneration (Cochran & Wozney 1999, MacNeil & Somerman 1999, Wikesjö & Selvig 1999, Jepsen et al. 2002, Needleman et al. 2002, AAP Position Paper 2005). Third, histologic data question whether the resulting tissues represent a true periodontal regeneration, because a cellular type of cementum with often a relatively loose connection to the underlying tooth structure is observed (Schroeder 1992, MacNeil & Somerman 1999, Grzesik & Narayanan 2002, Sculean et al. 2005, Bosshardt et al. 2006).

While the histological and clinical healing outcomes following these regenerative procedures are well documented in the literature, little is known about the healing dynamics at the cellular and molecular level during the regeneration process itself (Somerman et al. 1999, Zeichner-David 2006). Periodontal regeneration is a very complex wound-healing process requiring an exactly coordinated interaction of the cells of two different hard (cementum, bone) and two different soft tissues (gingiva, PDL). Whether the damaged tissues heal by regeneration or repair depends on the availability of the right cells and the signals and environment necessary to recruit and stimulate these cells. While the signals are provided by diffusible factors (e.g. growth factors, cytokines), the extracellular matrix (ECM) regulates how the cells respond to these signals (Grzesik & Narayanan 2002). The temporal expression of key ECM components is essential for the regeneration of periodontal tissues (Grzesik & Narayanan 2002). The development in future of innovative regenerative therapeutic strategies would ideally facilitate a predictable complete regeneration of all kinds of periodontal defects. This will require a better understanding of the precise interaction between the involved cells and the ECM proteins surrounding them.

Most of the histological studies in animals and humans have been limited to morphologic and histomorphometric aspects of periodontal healing outcomes. A limited number of immunohistolochemical investigations evaluating the regenerated tissues have shown the presence of collagen types I and III (Col-I and Col-III), vitronectin, fibronectin (FN), bone morphogenetic proteins-2, -4, -7, osteopontin (OPN), and bone sialoprotein (BSP) (Pritlove-Carson et al. 1992, Amar et al. 1995, 1997, Matsuura et al. 1995, Ivanovski et al. 2000, Sculean et al. 2002, 2003). Because in most of these studies tissue specimens were analysed only at a certain time point (Amar et al. 1997, Ivanovski et al. 2000), little is known about the temporal expression pattern of these ECM proteins during the periodontal wound-healing process. Furthermore, most of those studies did not include controls, i.e. open-flap debridement (OFD). Consequently, it is not known whether the regenerative therapy methods available change the temporal and spatial expression of ECM molecules compared with OFD facilitating the restoration of periodontal tissues.

For this reason, the aim of the present study was to assess the histological and immunohistochemical characterization of the temporal and spatial expression pattern of important ECM components during the wound-healing process in naturally occurring canine class II furcation defects following GTR therapy compared with OFD alone. Different bioresorbable and non-resorbable GTR membranes were used to analyse the possible influence of the materials and their degradation on the cell and tissue reactions. Five ECM proteins, characteristic for the hard and soft periodontal tissues, were analysed: Col-I, Col-III, FN, OPN and BSP.

Col-I and Col-III are the major constituents of all periodontal tissues and essential in establishing their structural and physiological integrity. FN, which originates from the serum and resident cells, plays an important role in wound repair by facilitating cell adhesion, spreading, and migration within the ECM. OPN and BSP are non-collagenous glycoproteins, which are secreted at different stages of osteogenesis and cementogenesis. Both proteins seem to have a unique distribution within the periodontium and accumulate predominantly at the hard tissue interfaces (MacNeil et al. 1995a, b, Boskey 1996, Bartold & Narayanan 1998, Ganss et al. 1999, Somerman et al. 1999, Sodek et al. 2000, Grzesik & Narayanan 2002).

Material and Methods

Study design

This study was designed to analyse the expression of selected ECM components during the periodontal wound-healing process in canine class II furcation defects 2, 4, and 8 weeks as well 3, 6, and 12 months after GTR therapy. The protocol of this animal study was approved by the Animal Welfare Committee of the University of Texas at Houston Health Science Center, Houston, TX, USA. The study was performed at the University of Texas at Houston Health Science Center in accordance with the NIH Guide for the Care and Use of Laboratory Animals.

Animal and defect selection

The study included 21 systemically healthy female beagle dogs, which were purchased from two federally licensed dealers (Harland Sprague–Dawley, Indianapolis, IN, USA, and Marshall Farms, Northrose, NY, USA). The age of the animals was 5–8 years and their body weight was 9.8–17.2 kg. All dogs showed advanced periodontal disease with naturally occurring buccal class II furcation defects at the mandibular second, third, and fourth pre-molars.

© 2007 The Authors. Journal compilation © 2007 Blackwell Munksgaard

Therapeutic procedure

After being housed for 2 weeks, the teeth of all dogs were thoroughly scaled and root planed. For this purpose, the animals were subjected to general anaesthesia using an initial intra-venous injection of Pentothal (17 mg/kg; Pentothal, Abott Laboratories, North Chicago, IL, USA), followed by gas anaesthesia (1–2% isoflurane/O_2, Isothesia, Burns Veterinary Supply, Rockville Centre, NY, USA). Thereafter, plaque control was maintained by tooth brushing and topical application of a 0.12% chlorhexidine solution (Peridex, Procter&Gamble, Cincinnati, OH, USA) every other day.

Two weeks following root instrumentation, each animal was anaesthetized as already described. Additional analgesia and bleeding reduction was achieved by local anaesthesia in the wound region (2% Xylocain with Epinephrin 1:500 000 Astra Pharmaceutical Products, Westborough, MA, USA). Following sulcular incisions, buccal and lingual mucoperiosteal flaps were elevated in the mandibular pre-molar regions. Vertical-releasing incisions were avoided to not compromise the flap vascularization. The extension of the naturally occurring buccal class II furcation defects of the left and right second, third, and fourth pre-molars was minimally standardized using rotating instruments and a periodontal probe. Thereafter, the periodontal defects were thoroughly scaled and planed using hand instruments (Gracey curettes, HuFriedy, Chicago, IL, USA) and rotating instruments (Perioset diamond burs, Intensiv, Viganello, Switzerland). Notches were placed in the roots and the furcation roof along the residual lingual bone, serving as landmarks for the histological evaluation indicating the most lingual extent of the furcation defect. Then, each of the second and fourth pre-molars was randomized for GTR therapy with one of the following membrane materials: polydioxanon (PDS) (Mempol, Ethicon, Norderstedt, Germany), polylactic acid (PLA) (Guidor Bioabsorbable Matrix Barrier, Guidor, Huddinge, Sweden), collagen (COL) (BioGide, Osteohealth, Shirley, NY, USA), or expanded polytetrafluoroethylene (e-PTFE) (GoreTex Periodontal Material, Gore, Flagstaff, AZ, USA). Each membrane was adjusted to cover the buccal entrance of the furcation lesion and 3 mm of the adjacent bone. As an internal negative control, both third pre-molars were treated by conventional OFD alone. Basal periosteal-releasing incisions were followed by coronal flap repositioning to obtain primary membrane coverage. The mucoperiosteal flaps were secured with interproximal modified horizontal matress sutures (CV-5, Gore), which were removed 2 weeks after surgery. For peri- and post-operative infection prophylaxis, systemic doxycycline (50 mg/day doxycycline hyclate capsule, Mutual Pharmaceuticals, Philadelphia, PA, USA) was given for 14 days (50 mg/day), starting 1 day before surgery (100 mg/day). In addition, analgesics (buprenorphinhydrochlorid, Buprenex, Reckitt & Colman Pahrmaceuticals, Richmond, VA, USA) were administered subcutanously for 2 days to minimize post-surgical discomfort. For the residual duration of the study, the dogs were fed soft food and water to protect the wound area from mechanical trauma. The plaque control regimen was continued as described above.

In 12 animals, which were scheduled for healing periods up to 8 weeks, the e-PTFE membranes remained in situ. In the other nine animals, the non-resorbable membranes were surgically removed 6 weeks after implantation. For this purpose, a split-thickness facial mucoperiosteal flap was reflected to remove the barrier. Afterwards, the flaps were positioned coronally and sutured. The sutures were retrieved after 1–2 weeks.

Tissue preparation

Histologic specimens were obtained 2, 4, and 8 weeks (four dogs each) as well as 3, 6, and 12 months (three dogs each) after GTR surgery. For this purpose, the animals were sacrificed by exsanguination under gas anaesthesia, followed by perfusion with 10% buffered formalin through the carotid arteries. Biopsies, comprising left or right mandibular segments with the second, third, and fourth pre-molars, were fixed in 10% buffered formalin for 24 h. Then, to improve fixation, these segments were cut in smaller parts, each containing only one tooth with its surrounding periodontal tissues, and fixed for another 24 h. Furthermore, five periodontally healthy maxillary second or third pre-molars with untreated pristine furcation areas were obtained for control purposes.

All specimens were decalcified in 5% neutral-buffered EDTA using a magnetic stirrer at 4°C. The EDTA solution was changed every other day. The endpoint of decalcification was determined radiographically. The biopsies were dehydrated through a graded series of ethanols and chloroform and then embedded in low melting point (56°C) paraffin (Paraplast, Oxford Labware, St Louis, MO, USA). Bucco-lingual serial sections were prepared at a thickness of 7–8 μm and collected on commercially available positively charged glass slides (Superfrost Plus, Fisher Scientific, Fair Lawn, NJ, USA). The sections were dried on a heating plate (Fisher Scientific) at 45°C for 48 h to increase tissue adherence to the slides. Representative sections were stained with Harris' haematoxylin and eosin (H&E) for conventional histological assessment.

Immunohistochemical procedures

Immunohistochemical labelling of ECM components was performed using the avidin–biotin–complex (ABC) method (Hsu et al. 1981) as described previously (Christgau et al. 1998). Representative sections taken from the central part of the defects were deparaffinized in xylene (EM Science; Gibbstown, NJ, USA) and re-hydrated through a descending series of ethanol concentrations. Unless otherwise mentioned, each incubation step during the immunohistochemical procedure was performed in a humidified chamber at room temperature (24°C) and was followed by thorough rinsing in 0.01 M Dulbecco's phosphate-buffered saline (PBS; Irvine Scientific, Santa Ana, CA, USA) three times for 5 min.

Endogeneous peroxidase activity was blocked by treating the sections with 0.3% hydrogen peroxide (Sigma, St Louis, MO, USA) in methanol for 30 min. This was followed by an enzymatic digestion with hyaluronidase (4000 U/ml; bovine testicular, Sigma) for 30 min. to expose the antigen structures under investigation. Afterwards, non-specific protein binding was blocked by incubation with 0.01 M PBS containing 10% normal goat serum (Vector Laboratories, Burlingame, CA, USA) for 30 min. Before one of the following primary antibodies was applied (Table 1), excess buffer was only blotted and rinsing with PBS was avoided: (a) polyclonal rabbit anti-bovine Col-I antibody (Fisher et al.

© 2007 The Authors. Journal compilation © 2007 Blackwell Munksgaard

Table 1. Polyclonal and monoclonal antibodies used for the immunohistochemical tissue analysis

Specificity*	Dilution	Origin of antigen	Clone	Host	Molecular specificity	Commercial source	References
Collagen type I	1:1500	Bovine	Polyclonal	Rabbit	$\alpha I(1)$ amino-propeptide	LF-9 (L. Fisher, NIH)	Fisher et al. (1987a, 1995)
Collagen type III	1:100	Human	IE7-D7	Mouse	Epitope near the N-terminal end	Biodesign #M43675M	Werkmeister & Ramshaw (1988, 1989), Werkmeister et al. (1989)
Fibronectin	1:3000	Human	Polyclonal	Rabbit	Plasma-fibronectin	Dako #A0245	D'Ardenne et al. (1986), Kirkpatrick & D'Ardenne (1984)
Bone sialoprotein	1:500	Human	Polyclonal	Rabbit	Human bone BSP	LF-6 (L. Fisher, NIH)	Bianco et al. (1993), Fisher et al. (1987b, 1995)
Osteopontin	1:500	Human	Polyclonal	Rabbit	Recombinant amino half ending at thrombin site	LF-124 (L. Fisher, NIH)	Fisher et al. (1995), Young et al. (1990)

*Specificity according to manufacturer's specifications.
BSP, bone sialoprotein.

Table 2 Immunoreactivity and staining intensity of the antibodies in the canine periodontal tissues

	Collagen type I	Collagen type III	Fibronectin	Bone sialoprotein	Osteopontin
Bone					
Osteoblasts	++++	0	++	++	0
Osteocytes	++	0	+	++	+
Osteoclasts	0	0	0	0	++++
Osteoid/new woven bone	+++	0	++	+++	+++
Extrinsic fibres	0	++	0	0	0
Old bone (lamellar bone)	+	0	+	+	+
Growth lines/reversal lines	0	0	0	+++	++
Root cementum					
Cementoblasts	+++	0	++	++/+++	+
Cementocytes	++	0	+	++	+
Odontoclasts	0	0	0	0	++++
Interface old/new cementum	0	0	+	++/+++	++/+++
Interface new cementum/PDL	0	0	0	++	++
Cementoid/new cementum	+++	0	+++	+++	+++
Old cementum	+	+	+	+	+
Extrinisic fibres	+	+++	0	0	0
Periodontal ligament					
Principal fibres	+++	++++	+	0	0
Ground substance	+++	+	+++	0	0
Fibroblasts	+++	0	++	0	0
Gingival connective tissue					
Fibroblasts	++++	0	++	0	0
Fibres	+++	+++	++	0	0
Ground substance	+++	+	+++	0	0
Dentogingival fibres	++	+++	+	0	0

Subjective scale of staining intensity: 0, no staining; +, weak staining; ++, moderate staining; +++, strong staining; ++++, very strong staining (dark brown, almost black).

1987a); (b) monoclonal mouse anti-human Col-III antibody (Werkmeister & Ramshaw 1988, 1989, Werkmeister et al. 1989); (c) polyclonal rabbit anti-human FN antibody (Kirkpatrick & D'Ardenne 1984, D'Ardenne et al. 1986); (d) polyclonal rabbit anti-human BSP antibody (Fisher et al. 1987b, Bianco et al. 1993); and (e) polyclonal rabbit anti-human OPN (Young et al. 1990). All antibody dilutions were prepared in 0.01 M PBS containing 5% normal goat serum. The incubation time was 1 h for the polyclonal antibodies (Col-I, FN, BSP, OPN) and 2 h for the monoclonal mouse antibody (Col-III).

Thereafter, the sections were treated sequentially with biotinylated goat anti-rabbit IgG (1:200) or goat anti-mouse IgG (1:200) (Vector Laboratories) and the avidin–enzyme complex (Vectastain Elite, Vector Laboratories). These treatments were followed by standardized development in 3,3′-diaminobenzidine (DAB; Vector Laboratories). The sections were lightly counterstained with Harris's modified haematoxylin (Fisher Scientific). Immunohistochemical staining of the ECM expression and periodontal wound-healing dynamics were assessed using a light microscope (Olympus BX40F-3, Olympus Optical, Tokyo, Japan).

For comparison of immunoreactivities of the individual antibodies, the labelling intensity of the tissue components was scored on the following scale of 0 to ++++ using subjective criteria: ''0'' = no staining, ''+'' = weak staining (minimally detectable), ''++'' = moderate staining, ''+++'' = strong staining, and ''++++'' = very strong staining (dark brown, almost black) (Table 2).

Controls for immunohistochemical staining

Negative control sections were treated by replacement of the primary antibodies either with pre-immune rabbit IgG (1:8000) (Dako Corporation, Carpinteria, CA, USA), pre-immune mouse $IgG_{1/2}$ (1:36) (Dako Corporation), or 0.01 M PBS alone. Negative controls were included in each experiment.

Results

Table 2 summarizes the immunoreactivity and staining intensity of all antibodies, which were used in the

© 2007 The Authors. Journal compilation © 2007 Blackwell Munksgaard

experiments, in canine periodontal tissues. For orientation purposes, Fig. 2a gives an overview of an entire class II furcation defect sectioned in the bucco-lingual plane. None of the negative controls showed any immunohistochemical staining (Fig. 2b).

Distribution of ECM components in pristine furcation areas

In pristine maxillary furcation areas, the gingival connective tissue revealed immunostaining for Col-I (Fig. 1b), Col-III (Fig. 1d, h), and FN (Fig. 1i). The strongest FN expression was found along the epithelial basement membrane and around chronic inflammatory infiltrates (Fig. 1i). While Col-I was relatively evenly distributed (Fig. 1b), Col-III was found mainly in the subepithelial connective tissue (Fig. 1h).

The PDL was immunopositive for Col-I (Fig. 1c), Col-III (Fig. 1d–f), and FN (Fig. 1i). PDL fibroblasts showed a strong expression of Col-I. Col-III appeared to be limited mainly to the dentogingival and principal PDL fibres (Fig. 1e, f). Neither BSP nor OPN were found in the PDL (Fig. 1j, k, m).

The extrinsic fibres (Sharpey fibres) of the root cementum stained for Col-III (Fig. 1f), while the cementum matrix itself was immunopositive for Col-I, FN, BSP (Fig. 1j, k), and OPN (Fig. 1m). The cytoplasm of the cementocytes stained for FN, Col-I, and BSP, but not for OPN and Col-III. The interfaces between cementum and dentin as well as between cementum and PDL showed a strong linear BSP expression (Fig. 1j, k).

The mineralized inter-radicular bone revealed only weak staining for Col-I (Fig. 1b, c), FN (Fig. 1i), BSP (Fig. 1j, l), and OPN (Fig. 1n). Col-III was only found in the fibres inserting from the connective tissue (Fig. 1g). The cytoplasm of osteocytes contained Col-I and BSP (Fig. 1c, j, l), while osteoclasts expressed mainly OPN. The reversal lines of the bone matrix revealed strong staining for BSP (Fig. 1l) and OPN (Fig. 1n, o). In general, the strongly mineralized cementum and bone matrix showed a very weak immunostaining, possibly due to antigen masking by the minerals.

Periodontal wound healing following GTR and OFD therapy

Figure 2c, d show examples of the typical healing outcomes in OFD- and GTR-treated sites under ideal healing conditions. The majority of OFD sites were characterized by the ingrowth of a long junctional epithelium (LJE) and only a limited amount of regeneration, while most of the GTR-treated sites showed significant periodontal regeneration. An important finding was that despite these quantitative differences in regeneration, the general spatial and sequential expression patterns of the investigated ECM proteins were similar following GTR with different membranes and OFD therapy. For this reason, in the following, the key steps of periodontal wound healing are described independently of the therapy method used.

Formation of granulation tissue (GT) and active new connective tissue

Two weeks after surgery, most of the defect area was still occupied by immature, strongly vascularized, and infiltrated GT (Fig. 3a). Its stroma intensely stained for FN (Fig. 3b), while the staining for Col-I (Fig. 3c) and Col-III (Fig. 3d) was still very faint and limited to some isolated fibres. BSP and OPN were not found in the GT. The strongest FN staining was found in the perivascular areas, along the epithelial basement membrane and at the interface to the GTR membranes (Fig. 3b). After 2 weeks, the GT was separated from the residual bone surface by a band of dense, fibrous Col-I+ and FN+ connective tissue and from the tooth surface by a thin layer of loose Col-I+ and FN+ connective tissue (Fig. 3a, c). Thin Col-I and Col-III fibres projected into the GT, indicating the stepwise organization of the GT by the adjacent fibrous connective tissue starting from the bone and tooth surface.

Four weeks after surgery, most of the GT was replaced by fibrous connective tissue, which appeared much more mature compared with the 2-week situation. The stroma of the connective tissue stained positive for FN and Col-I (Fig. 3e), while Col-III fibres were found as soon as the inflammatory infiltrates disappeared (Fig. 3f). In the following months, the majority of the connective tissue matrix was continuously replaced by the new bone and the new PDL, leaving only a layer of gingival connective tissue staining for Col-I, Col-III, and FN.

Formation of new bone tissue

Two weeks after surgery, a strong remodelling process was found along the surfaces and in the superficial marrow spaces of the residual inter-radicular bone. Numerous multinucleated OPN+ osteoclasts caused superficial bone resorptions. The interface between the osteoclasts and the resorption surfaces stained strongly for OPN (Fig. 3g). The resorption process was followed by a strong expression of OPN and BSP along the old and new bone surfaces as well as in the new bone matrix (Fig. 3h, i, j). Although, in some specimens, the first trabeculae of osteoid and new woven bone could already be found after 2 weeks (Fig. 3i, k), major bone formation was found starting after 4 weeks of healing (Fig. 3m, n). It was striking that in most specimens, bone formation advanced faster along the root surface compared with the rest of the defect. The new bone matrix stained strongly for FN and Col-I. The osteocytes as well as the osteoblasts densely covering the bone surfaces strongly expressed Col-I (Fig. 3k, m, n), underlining the important role of Col-I in bone matrix formation. While the old bone matrix did not show Col-III staining, numerous Col-III fibres projecting from the adjacent connective tissue were embedded in the new bone matrix (Fig. 3l). Marginal areas of the newly formed osteoid and woven bone matrix as well as the reversal lines revealed a rather strong staining for OPN and BSP (Fig. 4a, b). Even after 6 months, the newly formed bone could be distinguished from the old bone by its stronger staining for BSP and OPN (Fig. 4c, d). The cytoplasm of the osteocytes embedded in the new bone matrix showed a strong expression of BSP.

Formation of new cementum

The sequence of the ECM expression during the cementum formation was very similar to that observed during bone formation. Again, after 2 weeks, zones of superficial resorption with multinucleated cells (''odontoclasts'') were found along the residual cementum and dentin of the furcation fornix. The cytoplasm of the odontoclasts and their interface to the tooth substance showed strong OPN staining (Fig. 4e). Starting from the residual PDL lingually of the notch, the superficial root resorption was followed by a strong OPN and BSP

© 2007 The Authors. Journal compilation © 2007 Blackwell Munksgaard

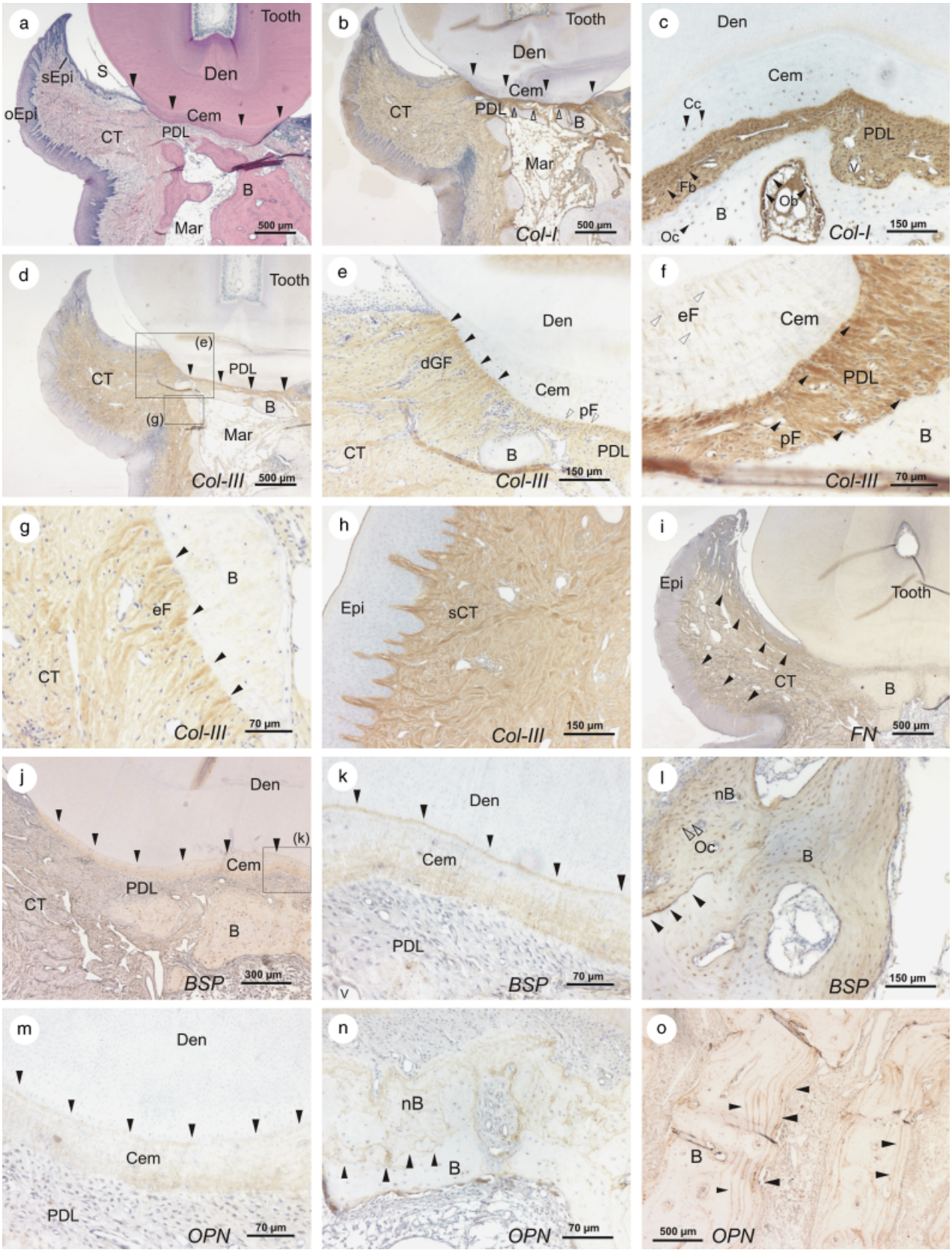

© 2007 The Authors. Journal compilation © 2007 Blackwell Munksgaard

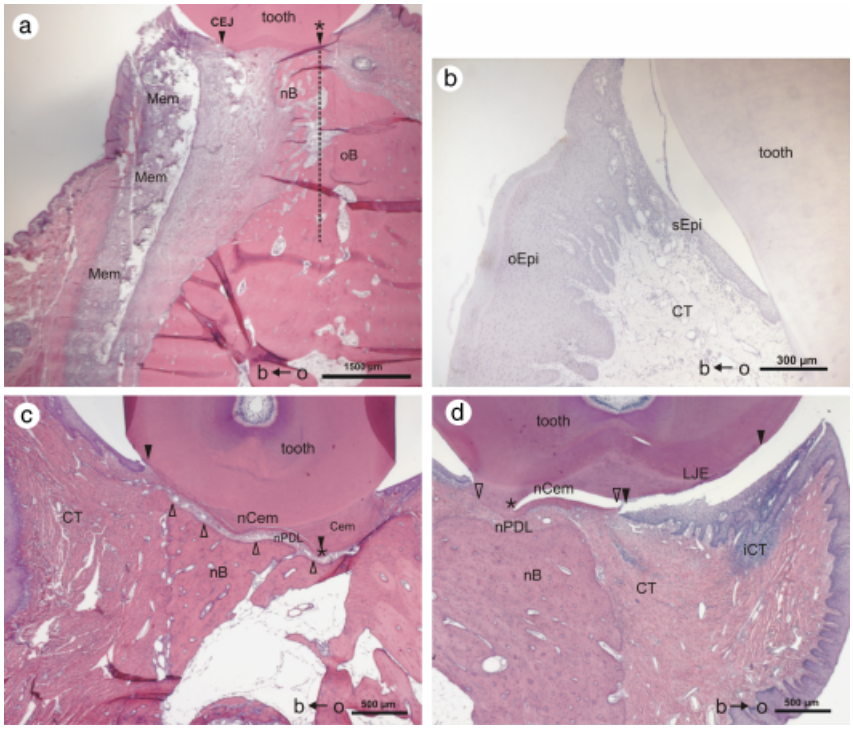

Fig. 2. (a) Overview of an entire class II furcation defect in a buccolingual section; the interrupted line delineates the most oral extent of the furcation defect; the buccal extent of the defect space is delineated by the membrane (mem). (b) Negative control: incubation with pre-immune mouse $IgG_{1/2}$; counterstaining with Harris's modified haematoxylin. (c, d) Healing outcomes in a guided tissue regeneration (GTR)-treated site (a) and an open-flap debridement (OFD)-treated site (b) haematoxylin and eosin (H&E): (c) 12-month healing result after GTR with a resorbable polydioxanon suture (PDS) membrane: almost complete regeneration with new cellular cementum (black arrows), new periodontal ligament (PDL) (white arrows), and new bone; (d) 6-month healing result after OFD: ingrowth of a long junctional epithelium (black arrows) and only little periodontal regeneration (white arrows). nPDL, new PDL; nCem, new cementum; nB, new bone; oB, old bone; CT, connective tissue; LJE, long junctional epithelium; iCT, infiltrated connective tissue; sEpi, sulcus epithelium; oEpi, oral epithelium; mem, membrane; CEJ, cementoenamel junction. *Delineates the oral border of the notch; o → b or b ← o: orientation in the oro-buccal direction.

expression along the interface between the residual tooth surface and the adjacent connective tissue (Fig. 4f, g). The next step was the condensation of a dense connective tissue matrix (cementoid) (Fig. 4h) along the tooth surface, which showed a strong staining for FN (Fig. 4i) and Col-I (Fig. 4j) and had direct contact with the residual PDL. At the entrance to the residual PDL space, a high cell density and activity was found (Fig. 4h). At this time, faint Col-III staining in the cementoid possibly indicated the formation and adhesion of the future extrinsic principal fibres (Fig. 4k). The cementoid matrix was densely covered by fibroblast-like cells, probably cementoblasts (Fig. 4h, j), which seemed to be responsible for the matrix formation along the root surface (Fig. 4j).

After 4 weeks, starting from the residual cementum lingual of the notch a thin layer of new cellular cementum was formed along the root surface (Fig. 4l, m). The thickness and buccal extension continuously increased until 12 months post-operatively, although the major part of the available tooth surface was covered by a new cementum layer already after 8 weeks (Figs 4n, o and 5a–d). The matrix of the new cementum revealed immunostaining for FN, Col-I, BSP, and OPN. A strong expression of BSP and OPN was found especially in the marginal areas of the new cementum. While the interface between new cementum and old/residual tooth substance (dentin or cementum) stained for both, BSP and OPN, the interface between new cementum and the adjacent connective tissue stained only for BSP (Figs 4n, o and 5a–d). In areas where an LJE was in contact with the root surface, no BSP or OPN staining was found along the interface (Fig. 4n). After 3 months, a new cementum layer reached from the notch at the border of the old PDL to the oral border of the LJE. During the subsequent months, the staining intensity for ECM proteins decreased with increasing

Fig. 1. Morphological and immunohistochemical staining for extracellular matrix components in pristine periodontal tissues (buccolingual sections): (a) overview of a periodonally healthy furcation area [haematoxylin and eosin (H&E)]; arrows delineate dentin/cementum interface; (b) anti-Col-I: strong expression in the PDL (white arrows); homogenous distribution in gingival connective tissue; black arrows delineate dentin/cementum interface; (c) anti-Col-I: homogenous distribution in the PDL; expression of Col-I by PDL Fb, Cc, Oc, and Ob; (d) anti-Col-III: staining in the PDL (arrows) and gingival connective tissue (e) anti-Col-III: high magnification of upper window in (d): strong Col-III staining in dentogingival (black arrows) and principal PDL (black arrows) fibres inserting into the cementum (f) anti-Col-III: intense staining of principal fibres (black arrows) in the PDL; note the faint staining of extrinsic fibres (white arrows) in the cementum; (g) anti-Col-III: high magnification of the lower window in (d): intense staining of extrinsic fibres (arrows) of the alveolar bone; (h) anti-Col-III: strong expression in subepithelial gingival connective tissue; (i)anti-FN: homogenous distribution of fibronectin in gingival connective tissue and PDL; stronger staining in subepithelial connective tissue (arrows); (j) anti-bone sialoprotein (BSP): overview of BSP staining in cementum and alveolar bone; arrows delineate the dentin/cementum interface; (k) anti-BSP: high magnification of the window in (j): granular BSP staining in cementum with strong expression at dentin/cementum interface (arrows); (l) anti-BSP: distribution of BSP in alveolar bone; intense staining of reversal lines (arrows) and stronger staining of new woven bone and osteocytes (white arrows); (m) anti-osteopontin (OPN): faint OPN staining in the cementum; arrows delineate dentin/cementum interface; (n) anti-OPN: note the stronger staining in the newly deposited woven bone and in the reversal lines (arrows); (o) anti-OPN: intense OPN expression in reversal lines of lamellar bone (arrows). Col, collagen; PDL, periodontal ligament; CT, connective tissue; sCT, subepithelial connective tissue; Epi, epithelium; Den, dentin; Cem, cementum; B, bone; nB, new bone; Mar, marrow; sEpi, sulcus epithelium; oEpi, oral epithelium; Cc, cementocytes; Fb, fibroblasts; Ob, osteoblasts; Oc, osteocytes; V, vessel; pF, principal fibres; dGf, dentogingival fibres; eF, extrinsic fibres.

© 2007 The Authors. Journal compilation © 2007 Blackwell Munksgaard

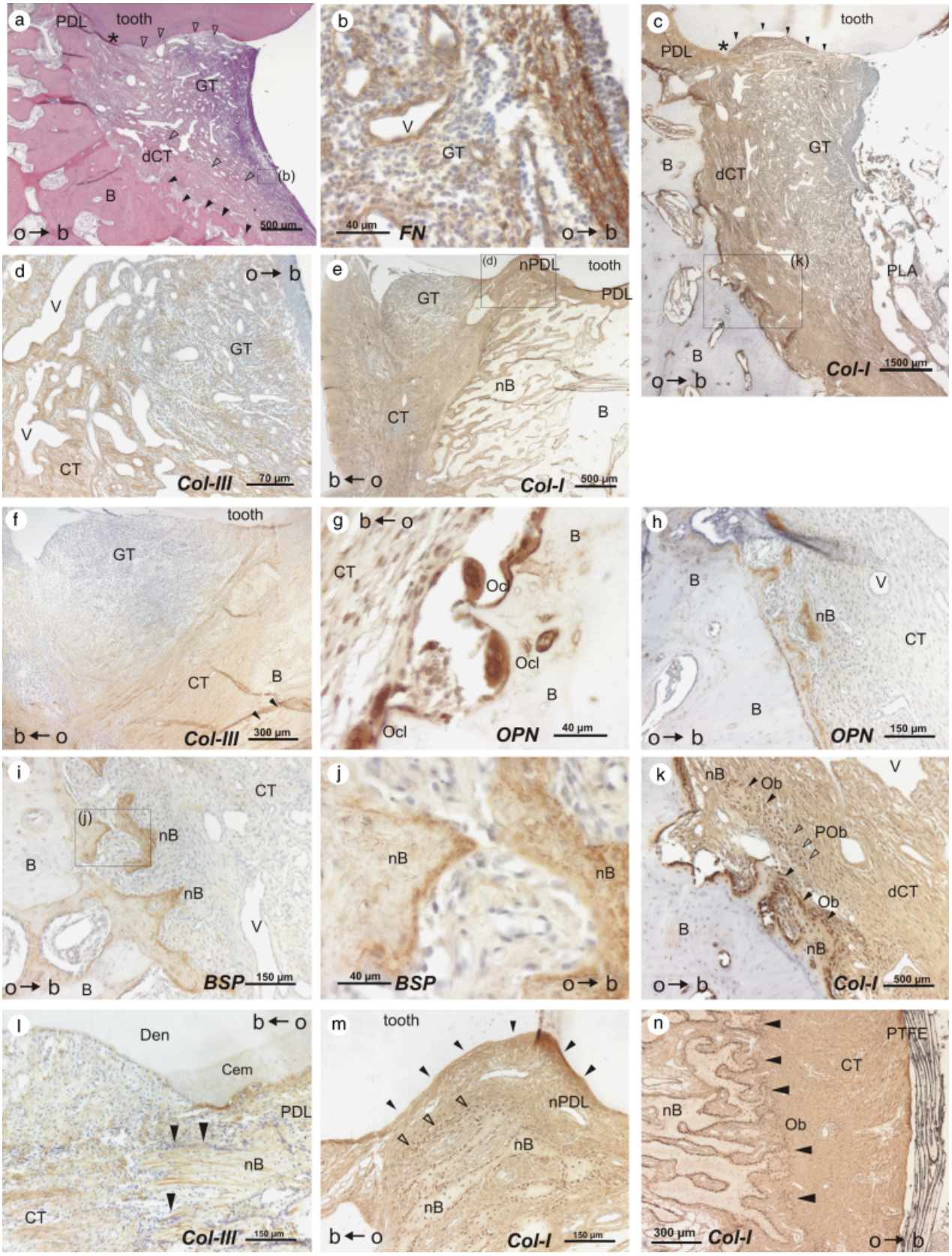

© 2007 The Authors. Journal compilation © 2007 Blackwell Munksgaard

degree of mineralization (Fig. 5d). An interesting finding was that cementogenesis preceded bone formation concerning its buccal extension and appeared to be independent of the osteogenesis (Figs 2a, b and 4n).

Formation of new PDL

Along with the osteo- and cementogenesis, the new PDL was formed, developing from the residual PDL lingually of the notch to the buccal side of the defect. Two weeks after surgery, only loose Col-I+ connective tissue was found between the root surface and the GT (Fig. 3c). The fibre orientation was mainly parallel to the root surface (Fig. 4j). At this time, only very few Col-I+ and Col-III+ fibres were already adhering perpendicular to the tooth surface (Fig. 5e, f), although they had not yet embedded in a new cementum and bone matrix. With the beginning of cementum deposition after 4 weeks, an increasing number of extrinsic collagen fibres inserted into the new cementum matrix (Fig. 5g, h), ending initially loosely in the adjacent connective tissue as dentogingival fibres. With increasing bone formation, these fibres also inserted into the new bone matrix forming the new PDL (Fig. 5i, m, n, o). After 3 months, in most specimens the new PDL space was completed. The new PDL showed staining for FN, Col-I, and Col-III. Col-I was found in the principal and secondary fibres, while Col-III was mainly limited to the Sharpey fibres and dentogingival fibres. Col-III staining was especially strong in the insertion area of the fibre bundles (Fig. 5n). The matrix of the PDL contained FN. Neither BSP nor OPN was found in the PDL.

Influence of wound stabilization and infection on ECM expression

While the general wound-healing dynamics were similar for the investigated therapy methods, the extension and the timing of ECM expression were clearly influenced by the degree of wound stabilization and inflammatory reactions caused by infections around the membranes. As an example, Fig. 6a–c illustrates this for the BSP expression after 4 weeks. Figure 6a shows the BSP expression along the tooth surface after 4 weeks in an inflammation-free and stable wound situation. Figure 6b shows a collapse of the gingival tissue and the ingrowth of a long LJE due to the lack of a space-maintaining wound stabilization in a site treated by a collagen membrane alone. Consequently, the BSP expression along the root surface was very limited. Figure 6c shows a strong inflammatory infiltrate around an exposed e-PTFE membrane. This massive infiltrate appeared to inhibit completely a BSP expression along the root surface.

Discussion

This study on periodontal wound-healing dynamics in naturally occurring canine class II furcation defects showed that periodontal regeneration can be obtained following GTR with different membranes and – at least in part – following OFD. The immunohistochemical analysis revealed well-defined, reproducible, tissue-specific temporal, and spatial expression patterns of key ECM proteins during the 12-month healing and regeneration process, leading to the formation of new cementum, PDL, and inter-radicular bone. The morphology and final staining pattern of the newly formed tissues were similar to those found in pristine healthy furcation areas.

Other immunohistochemical studies on periodontal wound healing in animals (Matsuura et al. 1995, Ivanovski et al. 2000, Kawaguchi et al. 2001) used surgically created, acute periodontal defect models without previous bacterial contamination. In contrast, we included only naturally occurring, chronically inflamed periodontal defects similar to the situation in humans. It is known that the integrity of cementum is chemically altered by disease (Grzesik & Narayanan 2002, Lao et al. 2006). Recently, Lao et al. (2006) could show a lack of BSP and OPN staining along previously diseased human root surfaces and discussed a possible negative influence on the ability for periodontal regeneration.

In contrast to a previous study on class III furcation defects (Matsuura et al. 1995), in the present study naturally occurring class II furcation defects were chosen. This defect model has

Fig. 3. (a–f) Formation of GT and active new connective tissue: (a) haematoxylin and eosin (H&E) overview of a class II defect showing the healing situation after 2 weeks: defect is mainly filled with infiltrated and strongly vascularized GT; note the zones of dense and loose connective tissue along the bone and tooth surface (white arrows), respectively; at the bottom of the defect first trabeculae of woven bone can be seen (black arrows); (b) anti-fibronectin (FN) after 2 weeks: high magnification of area similar to the window in (a): strong FN expression in GT, especially in the perivascular area and at the interface with the guided tissue regeneration (GTR) membrane (right margin); (e) overview of a class II defect: anti-Col-I after 2 weeks: strong staining in connective tissue along tooth (arrows) and bone surfaces (dCT); only weak staining in GT; note the very intense Col-I expression along the bone surface; (f) anti-Col-III after 2 weeks: relatively loose Col-III fibre network in new connective tissue; the GT contained only some isolated Col-III fibres; (g) anti-Col-I after 4 weeks: increased replacement of the GT by Col-I+ connective tissue originating from the bone and tooth surfaces; beginning formation of a new Col-I+ PDL; (h) anti-Col-III after 4 weeks [same specimen as in (e)]: while connective tissue along bone stains for Col-III, the granulation remains completely unstained; note some isolated extrinsic Col-III fibres in the bone (arrows); (g–n): formation of new bone: (i) anti-osteopontin (OPN) after 2 weeks: superficial resorption of residual alveolar bone by osteoclasts; note the strong OPN expression in the cytoplasm of the cells and their interface with the bone; (j) anti-OPN after 2 weeks: strong OPN expression along the bone surface and the new woven bone; (k) anti-bone sialoprotein (BSP) after 2 weeks: strong BSP expression along the bone surfaces and in the new bone matrix; only faint staining in the old bone (B); (l) anti-BSP: high magnification of window in (j): note the intense granular staining pattern of BSP in the new bone matrix and along the bone surface; (m) anti-Col-I after 2 weeks: high magnification of window in (c): strong Col-I expression in osteoblasts along the bone surface (black arrows) and in pre-osteoblasts (white arrows) in condensed connective tissue close to the bone surface; note the stronger staining of the new *versus* old bone matrix; (n) anti-Col-III after 2 weeks: extrinsic Col-III fibres (arrows) of the new woven bone ending in the adjacent connective tissue; (o) anti-Col-I after 4 weeks: strong Col-I expression by osteoblasts along new trabeculae of woven bone (white arrows); note strong staining of the fibres of the newly forming PDL (black arrows) (p) anti-Col-I after 4 weeks: dense Col-I+ connective tissue in direct contact with the PTFE membrane; active bone formation with bone trabeculae densely covered by osteoblasts strongly expressing Col-I (arrows). *Most oral extent of notch. Col, collagen; PDL, periodontal ligament; nPDL, new PDL; GT, granulation tissue; B, bone; nB, new bone; dCT, dense connective tissue; Ocl, osteoclast; Ob, osteoblast; POb, pre-osteoblast; V, vessel; PLA, polylactid acid membrane; PTFE, polytetrafluoroethylene membrane; o → b or b ← o, orientation in the oro-buccal direction.

© 2007 The Authors. Journal compilation © 2007 Blackwell Munksgaard

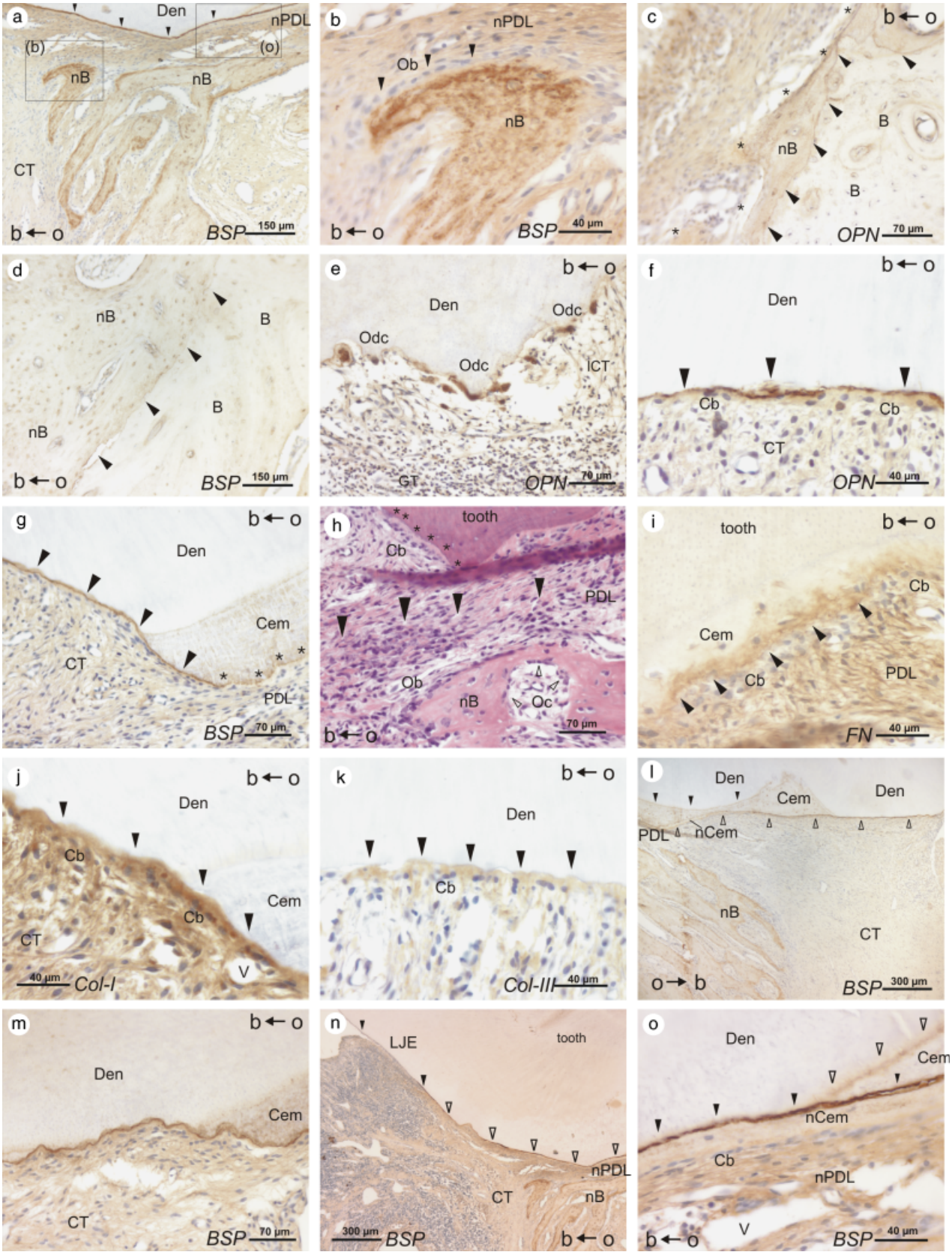

© 2007 The Authors. Journal compilation © 2007 Blackwell Munksgaard

already been described previously (Bogle et al. 1997). The class II defect required a histological evaluation in the buccolingual plane. As already discussed by Bogle et al. (1997), in class II furcation defects, sectioning in a mesiodistal plane may lead to some difficulties in interpreting the histologic results as it is difficult to be certain of the buccolingual point of origin for individual sections. Sections taken that are near an intact attachment apparatus (e.g. lingual defect wall in buccal class II furcation defects) may show more regenerative response than more buccal sections some distance from the intact periodontium, simply because of the proximity to regenerative cell precursors. Sectioning in a bucco-lingual plane allows an evaluation of the healing response of the entire class II defect from its most lingual extent to the buccal CEJ. This provides an accurate assessment of the overall regenerative response.

The advantage of using advanced class II furcation defects was the presence of a residual periodontium and residual bone wall at the most lingual extent of the defects. By using buccolingual sections, this defect model facilitated recognition of the residual periodontium as the origin of periodontal regeneration. Furthermore, on the bucco-lingual sections the GTR membranes, which defined the available space for regeneration, were visible.

For the assessment of the sequential ECM expression profile and the wound-healing dynamics, six different healing periods (2, 4, and 8 weeks, 3, 6, and 12 months) were considered similar to two previous investigations on periodontal wound-healing dynamics (Matsuura et al. 1995, Araujo et al. 1997). In contrast, other immunohistochemical studies on ECM expression included only one time point, making an assessment of the expression sequence difficult (Amar et al. 1995, 1997, Ivanovski et al. 2000, Kawaguchi et al. 2001, Sculean et al. 2002, 2003). To the best of our knowledge, this is the first study on periodontal wound-healing dynamics investigating the influence of GTR therapy on the temporal and spatial ECM expression profile compared with OFD therapy. The only other study on the temporal ECM profile (Matsuura et al. 1995) included only GTR-treated teeth.

In this context, it was an important observation that the basic wound-healing dynamics with regard to the spatial and temporal expression patterns of the investigated ECM proteins were similar following GTR with different membrane materials and OFD therapy. This seems to be plausible, because the GTR membranes exert mechanical effects providing cell-occlusion and space-maintaining wound stabilization without any active influence on the cell and matrix metabolism. This is confirmed by the 5-month findings in monkeys revealing a similar distribution of OPN, Col-I, and Col-III in sites treated by OFD and regenerative methods (Sculean et al. 2002). In contrast, Amar et al. (1997) found ECM proteins characteristic for bone and cementum formation only in GTR, but not in OFD-treated sites. However, they analysed only soft tissue biopsies from monkeys after 6 weeks, making an interpretation in the context of periodontal regeneration difficult.

Our study revealed four different stages of periodontal healing in the furcation defects: (1) initial defect fill with GT; (2) replacement of the GT by fibrous connective tissue and preparation of bone and root surfaces by transient resorptions; (3) formation of the mineralized tissues (bone, cementum) and the PDL by replacing the majority of the initial connective tissue volume; and (4) maturation process.

Corresponding to previous observations (Matsuura et al. 1995, Araujo et al. 1997), connective tissue formation occurred on the basis of a strongly FN+ GT serving as a scaffold for the ingrowth of Col-I and later of Col-III fibres. Owing to its strong expression in the inter-cellular and perivascular stroma and its numerous cellular- and matrix-binding sites, FN seemed to play an important role in the formation of a provisional matrix inducing the migration, adhesion, and differentiation of fibroblasts and endothelial cells (Yamada et al. 1985, Cho & Garant

Fig. 4. (a–d) Formation of new bone: (a) anti-bone sialoprotein (BSP) after 8 weeks: strong BSP expression at the margins of the new woven bone and along the interface between the dentin and new cementum (arrows); (b) anti-BSP after 8 weeks: high magnification of left window of (a): note strong granular BSP staining in new woven bone while osteoblasts (arrows) along the bone surface remain unstained; (c) anti-osteopontin (OPN) after 6 months: note the still significantly stronger OPN staining of the nB compared with the old B; intense staining of the reversal line (arrows); (d) anti-BSP after 6 months: stronger staining of new bone matrix compared with old bone; intense BSP staining of osteocytes in new bone and of the reversal line (arrows); (e–o): formation of new cementum: (e) anti-OPN after 2 weeks: superficial resorption of dentin matrix; note intense OPN staining of the cytoplasm of these cells and of their interface to the dentin; (f) anti-OPN after 2 weeks: intense OPN expression at the interface between dentin and new connective tissue (arrows); note the lining of fibroblast-like cells (cementoblasts?) close to OPN staining; (g) anti-BSP after 2 weeks: intense BSP staining of the interface between the tooth surface and new connective tissue in the defect area (arrows); note the significantly weaker staining of the residual cementum matrix and its interface to the residual PDL (*); (h) haematoxylin and eosin (H&E) overview after 2 weeks: condensed connective tissue matrix covered by cementoblasts along the tooth surface (*); trabeculae of new woven bone densely covered by osteoblasts; note the extremely high density of large fibroblast-like cells at the entrance to the old PDL (arrows): these cells may be highly active progenitor cells of cemento- and osteoblasts; (i) anti-fibronectin (FN) after 2 weeks: strong FN expression in the new condensed connective tissue matrix (arrows) along the tooth surface; (j) anti-Col-I after 2 weeks: very strong Col-I staining in the new condensed connective tissue matrix (arrows) along the dentin and cementum surface; (k) anti-Col-III after 2 weeks: faint Col-III staining in the connective tissue along the tooth surface indicating the beginning formation of new extrinsic fibres (arrows) of the new cementum; (l) anti-BSP after 4 weeks: strong staining along the interface between old tooth substance and nCem or adjacent connective tissue (white arrows); black arrows delineate interface between dentin and old cementum; (m) anti-BSP after 4 weeks: strong staining along the interface between old cementum/dentin and adjacent connective tissue; (n) anti-BSP after 8 weeks: strong BSP expression at the interface between dentin and new cementum or connective tissue (white arrows); note missing BSP expression in the area of the long junctional epithelium (between black narrows); (o) anti-BSP after 8 weeks. High magnification of right window of (a): strong BSP expression at the interface between new cementum and dentin/old cementum (black arrows); note relatively strong staining also at the interface between old cementum and dentin (white arrows). PDL, periodontal ligament; nPDL, new PDL; B, bone; nB, new bone; CT, connective tissue; ICT, infiltrated connective tissue; GT, granulation tissue; Den, dentin; Cem, cementum; nCem, new cementum; LJE, long junctional epithelium; Ocl, osteoclast; Ob, osteoblast; Odc, odontoclast; Cb, cementoblast; V, vessel; o → b or b ← o, orientation in the oro-buccal direction.

© 2007 The Authors. Journal compilation © 2007 Blackwell Munksgaard

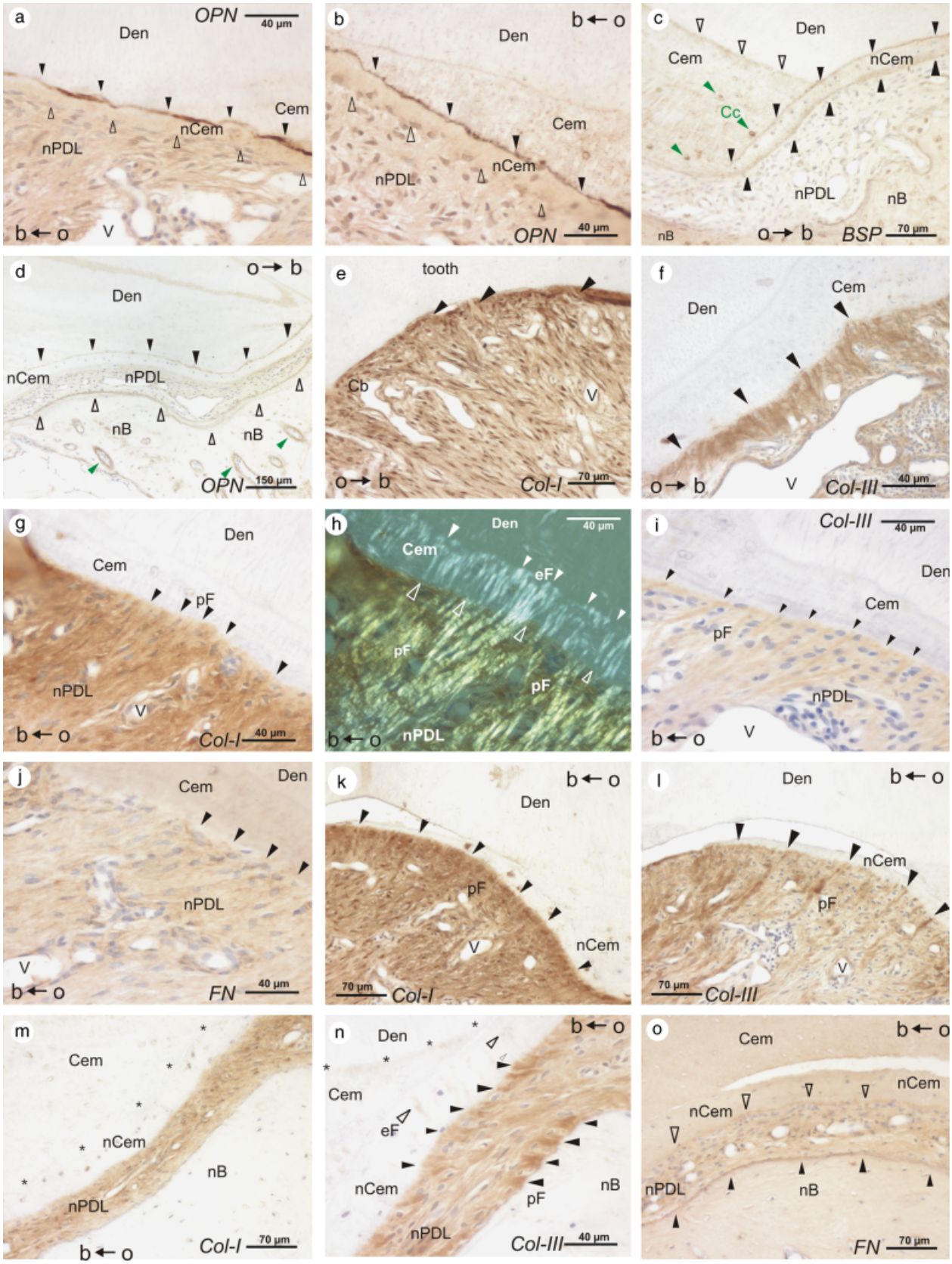

© 2007 The Authors. Journal compilation © 2007 Blackwell Munksgaard

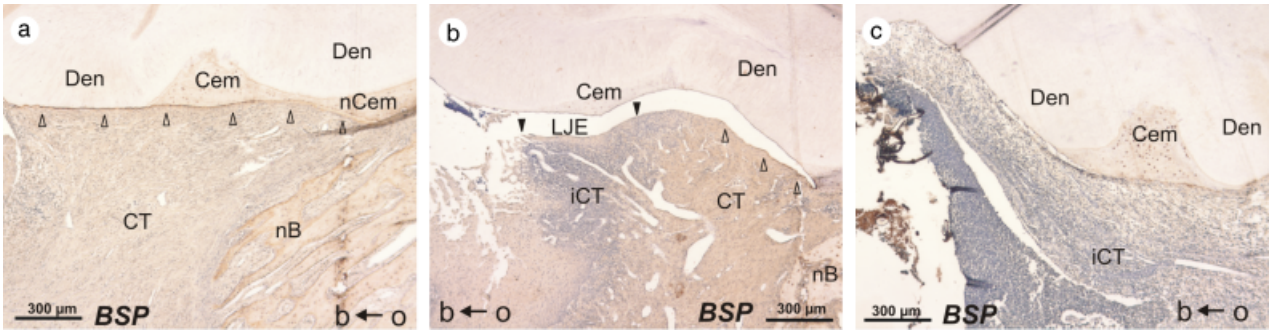

Fig. 6. Influence of wound stabilization and inflammatory reactions on matrix expression: (a) anti-bone sialoprotein (BSP) after 4 weeks: BSP expression along the entire exposed tooth surface (arrows) in a stable space-maintaining wound-healing situation free of inflammation; (b) anti-BSP after 4 weeks: collapse of gingival tissues into the defect area and formation of a LJE (black arrows) due to the insufficient wound stabilization by a collagen membrane; note the very limited area of tooth surface revealing BSP staining (white arrows); (c) anti-BSP after 4 weeks: the inflammatory infiltrate caused by an infection around an exposed PTFE membrane completely inhibited any BSP expression at the tooth surface. CT, connective tissue; iCT, infiltrated connective tissue; Cem, cementum; nCem, new cementum; nB, new bone; Den, dentin; LJE, long junctional epithelium; o → b or b ← o, orientation in the oro-buccal direction.

1989, Dean & Blankenship 1997). As described previously (Matsuura et al. 1995, Araujo et al. 1997), connective tissue formation started from the highly active areas along the tooth and bone surfaces, revealing a high density of Col-I-expressing fibroblasts. Compared with the FN and Col-I staining, we observed a delayed expression of Col-III in the new connective tissue. This seems to be in contrast to previous findings in skin wounds (Eckes et al. 2000) and periodontal wound healing (Ivanovski et al. 2000). It may be explained by the residual inflammatory infiltrates still found during early wound healing. In the past, it has been shown that gingival inflammation affects Col-III more than Col-I (Narayanan et al. 1985). Our findings are confirmed by previous in situ hybridization in healing periodontal tissues revealing a stronger Col-I than Col-III mRNA expression (Larjava et al. 1990).

As described previously (Schenk et al. 1994, Araujo et al. 1999), bone formation took place in three well-defined steps of desmal ossification: (a) formation of a transitional connective tissue matrix serving with its Col-I and Col-III fibres as a scaffold for the subsequent hard tissue formation; (b) formation of primary bone in the form of compact woven bone; and (c) transformation to lamellar bone with wider marrow spaces. The deposition of new bone matrix was preceded by an initial superficial resorption of the residual bone by osteoclasts strongly expressing OPN. By facilitating the adhesion to the mineralized substance, OPN seems to serve as a sealing substrate for the osteoclasts to establish a tight acidic environment for the decalcification process (Reinholt et al. 1990). The resorption was followed by a strong expression of OPN and BSP along the exposed old bone surface. Both proteins seem to be important factors for the chemoattraction, adhesion, and differentiation of osteoprogenitor cells from the adjacent connective tissue (McKee & Nanci 1996a, Romano et al. 1997, Saffar et al. 1997). Furthermore, there are indications that both proteins play an important role in the mineralization process (Cowles et al. 1998). An interesting

Fig. 5. (a–d) Formation of nCem: (a) anti-osteopontin (OPN) after 8 weeks: strong OPN expression at the interface between nCem and dentin/old Cem (black arrows); weaker staining of nCem matrix (white arrows); (b) anti-OPN after 8 weeks: strong OPN expression at the interface between nCem and dentin/old Cem (black arrows); weaker staining of nCem matrix (white arrows); (c) anti-bone sialoprotein (BSP) after 12 months: similar staining intensity of old and nCem; strong staining at the interface between dentin and old Cem (white arrows) and at the interfaces of the nCem with old Cem, dentin and periodontal ligament (PDL) (black arrows); staining of cementocytes in old Cem (green arrows); note cellular type of Cem; (d) anti-OPN after 12 months: OPN staining only at the interface between dentin and nCem (black arrows) as well as along the external (white arrows) and internal (green arrows) bone surfaces; bone and Cem matrix remains unstained; (e–o): formation of new periodontal ligament: (e) anti-Col-I after 2 weeks: already at this time some isolated Col-I+ fibre bundles with an orientation perpendicular to the tooth surface (arrows) could be seen in the area of the notch; (f) anti-Col-III after 2 weeks [same specimen as in (e)]: first Col-III fibres with an orientation perpendicular to the dentin surface (arrows) in the area of the notch; the fibres attach to the dentin surface without being invested in a nCem matrix yet; (g) anti-Col-I after 8 weeks: strong Col-I staining of the fibres in the new PDL space; note the principal fibres (arrows) perpendicularly inserting in the nCem matrix; (h) same specimen as in (g) under polarized light: birefringencies show principal fibres of the PDL; many fibres can be followed as extrinsic fibres from the PDL to the dentin (white arrows); the cellular mixed fibre Cem (between white and dark arrows) shows a high density of extrinsic fibres; (i) anti-Col-III after 8 weeks: strong Col-III staining of principal fibres (arrows) of the new PDL; (j) anti-fibronectin (FN) after 8 weeks: relatively homogenous FN staining in the new PDL; some stronger staining at the insertion sites of the principal fibres (arrows); (k) anti-Col-I after 3 months: strong Col-I staining of the entire new PDL; note the very intense staining of the principal fibres close to their insertion sites at the nCem (arrows) and of the PDL fibroblasts; (l) anti-Col-III after 3 months [similar area as in (k)]: strong Col-III staining in new principal fibres (arrows); (m) anti-Col-I after 12 months: strong Col-I staining of all PDL fibres; note that the new matured bone and Cem matrix remain largely unstained; *interface between new and old Cem; (n) anti-Col-III after 12 months: note the intense Col-III staining of the principal fibre bundles inserting in the Cem and bone matrix (arrows); in the nCem matrix some weak staining of extrinsic fibres (white arrows) can be seen; *interface between dentin and old Cem; (o) anti-FN after 12 months: homogenous distribution of FN in matrix of PDL, Cem and bone; stronger expression along the PDL interfaces with Cem (white arrows) and bone (black arrows). nPDL, new PDL; nB, new bone; Den, dentin; Cem, cementum; nCem, new cementum; Cc, cementocyte; Cb, cementoblast; pF, principal fibres; extrinsic fibres; V, vessel; o → b or b ← o, orientation in the oro-buccal direction.

© 2007 The Authors. Journal compilation © 2007 Blackwell Munksgaard

finding was that bone formation along the root surface preceded the bone fill of the residual defect, normally. A similar observation was made in class III furcation defects (Matsuura et al. 1995). This may confirm the hypothesis that tooth-supporting bone is formed by osteoblasts with an origin in the PDL (McCulloch 1995). The strong expression of BSP and OPN along the root surface possibly also had a chemotactic effect on osteoblasts of the PDL, causing an accelerated bone formation along the tooth surface. Ankylosis was probably prevented by OPN, which is supposed to have inhibitory effects on the mineralization process (Denhardt & Guo 1993, MacNeil et al. 1995a). As reported previously (Denhardt & Guo 1993, Ganss et al. 1999, Sodek et al. 2000), the new osteoid showed a strong expression of FN, Col-I, BSP, and OPN. Although not seen in old bone, numerous Col-III fibres inserting from the surrounding connective tissue were found in the osteoid and new bone matrix. These fibres seemed to serve as a transitory scaffold and guiding structure for the new bone formation. Similar observations were made in extraction sockets (Becker et al. 1986, 1989).

The formation of new root cementum and its adherence to the pathologically altered and treated root surface is regarded as the key event of periodontal regeneration by connecting the collagen fibres of the new PDL with the altered root surface (MacNeil & Somerman 1999, Grzesik & Narayanan 2002, Bosshardt et al. 2005). In the present study, bone and cementum formation showed several similarities concerning ECM protein expression and healing dynamics. The new cementum formation was also preceded by a superficial transient resorption of the residual dentin and root cementum by multinucleated giant cells, so-called odontoclasts. Similar to osteoclasts, a strong OPN expression was found in the cytoplasm of these cells and at their interface to the tooth surface. This resorptive activity, which has already been described previously (Frank et al. 1974, Nalbandian & Frank 1980, Aukhil et al. 1983, 1986, Araujo et al. 1996, Wikesjö & Selvig 1999, Bosshardt et al. 2005), is supposed to pre-condition the underlying dentin by exposing collagen fibres to facilitate a firm attachment of the new cementum matrix (Bosshardt et al. 2005, Graziani et al. 2005, Laurell et al. 2006). The primary event of new cementoid deposition was a strong accumulation of OPN and BSP along the root surface. This corresponds to previous observations in cementogenesis and cementum regeneration (Somerman et al. 1990, Bronckers et al. 1994, MacNeil et al. 1994, 1996, Matsuura et al. 1995, Bosshardt & Nanci 1998, Ivanovski et al. 2000, Kawaguchi et al. 2001, Bosshardt et al. 2005). Although the exact role of OPN in cementum formation is not yet known, it seems to promote cell attachment to the root surface. The new extrinsic fibres insert into this OPN-rich layer (McKee et al. 1996). Bosshardt et al. (2005) showed that the collagenous matrix of repair cementum in human deciduous teeth becomes integrated in an electron-dense zone labelling for BSP and OPN. OPN might suppress the mineralization process (MacNeil et al. 1995a). BSP seems to be responsible for the differentiation of pre-cementoblasts, their attachment to the root surface as well as the early mineralization of the cementum matrix (MacNeil et al. 1995a, Bartold & Narayanan 1998, Grzesik & Narayanan 2002). In our study, the origin of BSP and OPN could not be verified, because cellular staining was rather faint. It has been proposed that the deposition of BSP and OPN is part of the normal protein secretory sequence of cementoblasts that form repair cementum (Bosshardt et al. 1998, 2005, Nanci 1999). However, both non-collagenous proteins also circulate within the blood stream, and inflammatory cells such as macrophages produce OPN (McKee & Nanci 1996b, van den Bos et al. 1999). Thus, it is likely that proteins in tissue fluids also contribute to the accumulation of BSP and OPN on the denuded root surface. Although FN is found to be diffusely distributed in the cementum matrix, it was not particularly concentrated at the interface between dentin and regenerative cementum, corresponding to previous observations (Kawaguchi et al. 2001). Thus, it is unlikely that FN is involved in the initial adhesion events at the denuded root surfaces.

Already after 2 weeks, as an early stage of cementum deposition, the OPN and BSP expression along the root surface was followed by condensation of a dense connective tissue matrix staining intensely for FN and Col-I. Very soon, an increasing number of Col-III fibres inserted perpendicularly into the OPN and BSP+ interface, forming new extrinsic fibres. Similar to previous observations (Matsuura et al. 1995), after 4 weeks a thin layer of cellular cementum started to replace the preceding connective tissue matrix. An important observation was that all steps of new cementum formation always started at the interface to the old residual PDL. This clearly confirms that the residual PDL is the source of cementoblast progenitor cells responsible for the new cementum formation (Melcher 1976, McCulloch & Bordin 1991, Herr et al. 1995, Liu et al. 1997). BSP and OPN appeared to attract these cells and induce their spreading along the tooth surface (Saygin et al. 2000). In contrast to our findings, Araujo et al. (1997) found patches of new cementum, which initially had no contact to the old cementum. Another interesting observation of our study was that cementum formation seemed to be independent of the bone formation and preceded it. While most of the root surface was covered by new cementum already after 8 weeks, the thickness increased until 12 months after surgery. This increasing maturation confirms previous reports by Laurell et al. (2006) and Graziani et al. (2005). In contrast to their findings after GTR therapy in intra-bony defects in monkeys, we could not detect acellular extrinsic fibre cementum (Schroeder 1986). Even after 12 months, the new cementum revealed the characteristics of a cellular mixed fibre cementum (CMFC) at the furcation roof. However, according to the literature (Schroeder 1986) and our findings in pristine furcation areas, CMFC seems to be the predominant type of cementum naturally occurring in the furcation area. The new CMFC revealed staining for FN, Col-I, BSP, and OPN, while Col-III was limited to the extrinsic fibres. It has to be emphasized that in our study, despite the initial root resorption and the strong OPN/BSP expression, a gap between old and new cementum was often observed as described previously in the literature (Schroeder 1992, MacNeil & Somerman 1999, Grzesik & Narayanan 2002, Bosshardt et al. 2006). This may be possibly a problem of CMFC (Laurell et al. 2006).

Parallel to cementum and bone formation, the new PDL was formed, again starting from the residual PDL. In contrast to a previous study (Araujo et al. 1997), Col-I and Col-III fibres inserted already into the woven bone. Araujo et al. found PDL fibre insertion only in lamellar bone. As already shown in

© 2007 The Authors. Journal compilation © 2007 Blackwell Munksgaard

different species (Becker et al. 1991, Beertsen et al. 1997, Kapila et al. 1998), the new PDL contained Col-I, Col-III, and FN. Col-I was detected in the primary and secondary fibres, while Col-III staining was mainly limited to the principal fibres. Corresponding to previous studies (Ogata et al. 1995, Nohutcu et al. 1997, MacNeil et al. 1998), we could not detect OPN or BSP in the new and old PDL. This was in contrast to other studies (Matsuura et al. 1995, Ivanovski et al. 2000), which reported some BSP staining within the PDL in canines. Sculean et al. (2002) reported an abundant OPN staining in the new and original PDL.

The present paper has focused mainly on the basic wound-healing dynamics, which seems to be similar in sites treated by different GTR membranes and OFD therapy. However, it has to be emphasized that the amount of periodontal regeneration and the extension of ECM formation were significantly influenced by the quality and duration of space-maintaining wound stabilization and inflammatory reactions caused by infections in the defect area. As described previously (Haney et al. 1993, Sigurdsson et al. 1994), the importance of mechanical protection of the blood clot and GT as well as the cell-occlusion against epithelial cells became obvious. Especially in sites treated by OFD alone or by collagen membranes without any additional defect fillers, a collapse of the gingival connective tissue and the ingrowth of a LJE occurred very often. Consequently, the space available for the expression of key ECM proteins and for the restoration of periodontal tissues was significantly reduced. Furthermore, our results showed clearly the detrimental influence of inflammatory reactions caused by bacterial contamination of exposed GTR membranes on the regeneration process. They inhibited or delayed the formation of collagens as well as the expression of BSP and OPN along the root surfaces, which seem to be crucial for new cementum formation. This confirms recently published immunohistochemical findings (Lao et al. 2006), which also showed absence of BSP and OPN staining along pathologically exposed human cementum surfaces.

Conclusion

Within the limits of this study in canine class II furcation defects, the investigated ECM components were expressed in a clearly defined sequence characteristic for each of the periodontal tissues. In general, we could not find differences in the spatial expression pattern between GTR- and OFD-treated sites. However, the timing and quantity of ECM expression were significantly influenced by the degree of wound stabilization and by inflammatory reactions caused by infections. These descriptive findings may provide the framework for future studies aimed at the development of novel bioengineered scaffolds for periodontal regeneration.

Acknowledgements

The authors thank Gill Rittman, Norva Steward, Verna Hubbard (UTHHSC), and Johanna Christgau for their valuable help in the histological processing of our specimens. We are grateful to the veterinarians Dr. Chris Smith and Dr. Terry Blasdel, representing all coworkers of the Center for Laboratory Animal Medicine and Care (CLAMC, UTHHSC), for the excellent care for our animals. The authors thank Professor Larry Fisher (NIH) for generously providing the antibodies LF-9, LF-6, and LF-124.

References

AAP Position Paper (2005) Periodontal regeneration. *Journal of Periodontology* **76**, 1601–1622.

Amar, S., Chung, K. M., Nam, S. H., Karatzas, S., Myokai, F. & Van Dyke, T. E. (1997) Markers of bone and cementum formation accumulate in tissues regenerated in periodontal defects treated with expanded polytetrafluoroethylene membranes. *Journal of Periodontal Research* **32**, 148–158.

Amar, S., Petrungaro, P., Amar, A. & Van Dyke, T. E. (1995) Immunolocalization of bone matrix macromolecules in human tissues regenerated from periodontal defects treated with expanded polytetrafluoroethylene membranes. *Archives of Oral Biology* **40**, 653–661.

Araujo, M. G., Berglundh, T., Albrektsson, T. & Lindhe, J. (1999) Bone formation in furcation defects. An experimental study in the dog. *Journal of Clinical Periodontology* **26**, 643–652.

Araujo, M. G., Berglundh, T. & Lindhe, J. (1996) The periodontal tissues in healed degree III furcation defects. An experimental study in dogs. *Journal of Clinical Periodontology* **23**, 532–541.

Araujo, M. G., Berglundh, T. & Lindhe, J. (1997) On the dynamics of periodontal tissue formation in degree III furcation defects. An experimental study in dogs. *Journal of Clinical Periodontology* **24**, 738–746.

Aukhil, I., Pettersson, E. & Suggs, C. (1986) Guided tissue regeneration. An experimental procedure in beagle dogs. *Journal of Periodontology* **57**, 727–734.

Aukhil, I., Simpson, D. M. & Schanberg, T. V. (1983) An experimental study of new attachment procedure in beagle dogs. *Journal of Periodontal Research* **18**, 643–654.

Bartold, P. M. & Narayanan, A. S. (1998) *Periodontal Connective Tissues*, 1st edition. Chicago: Quintessence.

Becker, J., Schuppan, D., Benzian, H., Bals, T. H. E. G., Cantaluppi, C. & Reichart, P. (1986) Immunohistochemical distribution of collagens types IV, V, and VI and of procollagens type I and III in human alveolar bone and dentine. *Journal of Histochemistry and Cytochemistry* **34**, 1417–1429.

Becker, J., Schuppan, D., Rabanus, J.-P., Rauch, R., Niechoy, U. & Gelderblom, H. R. (1991) Immunoelectron microscopic localization of collagens type I, V, VI and of procollagen type III in human periodontal ligament and cementum. *Journal of Histochemistry and Cytochemistry* **39**, 103–110.

Becker, J., Schuppan, D., Selle, C., Bunte, T. & Reichart, P. (1989) Immunhistochemische untersuchungen zum aufbau der extrazellulären bindegewebsmatrix während der wundheilung im knochen. *Zahnärztliche Implantologie* **V**, 205–210.

Beertsen, W., McCulloch, C. A. G. & Sodek, J. (1997) The periodontal ligament: a unique, multifunctional connective tissue. *Periodontology 2000* **13**, 20–40.

Bianco, P., Riminucci, M., Silvestrini, G., Bonucci, E., Termine, J. D., Fisher, L. W. & Robey, P. G. (1993) Localization of bone sialoprotein (BSP) to Golgi and post-golgi secretory structures in osteoblasts and to discrete sites in early bone matrix. *Journal of Histochemistry and Cytochemistry* **41**, 193–203.

Bogle, G. C., Garrett, S., Stoller, N. H., Swanbom, D. D., Fulfs, J. C., Rodgers, P. W., Whitman, S., Dunn, R. L., Southard, G. L. & Polson, A. M. (1997) Periodontal regeneration in naturally occurring class II furcation defects in beagle dogs after GTR with bioabsorbable barriers. *Journal of Periodontology* **68**, 536–544.

Boskey, A. L. (1996) Matrix proteins and mineralization: an overview. *Connective Tissue Research* **35**, 357–363.

Bosshardt, D. D., Degen, T. & Lang, N. P. (2005) Sequence of protein expression of bone sialoprotein and osteopontin at the developing interface between repair cementum and dentin in human deciduous teeth. *Cell and Tissue Research* **320**, 399–407.

Bosshardt, D. D. & Nanci, A. (1998) Immunolocalization of epithelial and mesenchymal matrix constituents in association with inner enamel epithelial cells. *Journal of Histochemistry and Cytochemistry* **46**, 135–142.

Bosshardt, D. D., Sculean, A., Donos, N. & Lang, N. P. (2006) Pattern of mineralization after regenerative periodontal therapy with

© 2007 The Authors. Journal compilation © 2007 Blackwell Munksgaard

enamel matrix proteins. *European Journal of Oral Sciences* **114** (Suppl. 1), 225–231.

Bosshardt, D. D., Zalzal, S., McKee, M. D. & Nanci, A. (1998) Developmental appearance and distribution of bone sialoprotein and osteopontin in human and rat cementum. *The Anatomical Record* **250**, 13–33.

Bronckers, A. L. J. J., Farach-Carson, M. C., Van Waveren, E. & Butler, W. T. (1994) Immunolocalization of osteopontin, osteocalcin, and dentin sialoprotein during dental root formation and early cementogenesis in the rat. *Journal of Bone and Mineral Research* **9**, 833–841.

Caffesse, R. G., Dominguez, L. E., Nasjleti, C. E., Castelli, W. A., Morrison, E. C. & Smith, B. A. (1990) Furcation defects in dogs treated by guided tissue regeneration. *Journal of Periodontology* **61**, 45–50.

Caffesse, R. G., Nasjleti, C. E., Morrison, E. C. & Sanchez, R. (1994) Guided tissue regeneration: comparison of bioabsorbable and non-absorbable membranes. Histologic and histometric study in dogs. *Journal of Periodontology* **65**, 583–591.

Caffesse, R. G., Smith, B., Castelli, W. & Nasjleti, C. (1988) New attachment achieved by guided tissue regeneration in beagle dogs. *Journal of Periodontology* **59**, 589–594.

Camelo, M., Nevins, M. L., Schenk, R. K., Simion, M., Rasperini, G., Lynch, S. E. & Nevins, M. (1998) Clinical, radiographic, and histologic evaluation of human periodontal defects treated with Bio-Oss and Bio-Gide. *International Journal of Periodontics and Restorative Dentistry* **18**, 321–331.

Cho, M.-I. & Garant, P. R. (1989) Radioautographic study of (3H) mannose utilization during cementoblast differentiation, formation of acellular cementum, and development of periodontal ligament principal fibers. *The Anatomical Record* **223**, 209–222.

Christgau, M., Caffesse, R. G., Newland, J. R., Schmalz, G. & D'Souza, R. N. (1998) Characterization of immunocompetent cells in the diseased canine periodontium. *Journal of Histochemistry and Cytochemistry* **46**, 1443–1454.

Christgau, M., Moder, D., Hiller, K. A., Dada, A., Schmitz, G. & Schmalz, G. (2006a) Growth factors and cytokines in autologous platelet concentrate and their correlation to periodontal regeneration outcomes. *Journal Clinical Periodontology* **33**, 837–845.

Christgau, M., Moder, D., Wagner, J., Gläßl, M., Hiller, K. A., Wenzel, A. & Schmalz, G. (2006b) Influence of autologous platelet concentrate on healing in intrabony defects following GTR therapy. A randomized prospective clinical split-mouth study. *Journal Clinical Periodontology* **33**, 908–921.

Cochran, D. L. & Wozney, J. M. (1999) Biologic mediators for periodontal regeneration. *Periodontology 2000* **19**, 40–58.

Cowles, E. A., DeRome, M. E., Pastizzo, G., Brailey, L. L. & Gronowicz, G. A. (1998) Mineralization and the expression of matrix proteins during in vivo bone development. *Calcified Tissue International* **62**, 74–82.

D'Ardenne, A. J., Kirkpatrick, P., Wells, C. A. & Davies, J. D. (1986) Laminin and fibronectin in adenoid cystic carcinoma. *Journal of Clinical Pathology* **39**, 138–144.

Dean, J. W. & Blankenship, J. A. (1997) Migration of gingival fibroblasts on fibronectin and laminin. *Journal of Periodontology* **68**, 750–757.

Denhardt, D. T. & Guo, X. (1993) Osteopontin: a protein with diverse functions. *FASEB Journal* **7**, 1475–1482.

Eckes, B., Zigrino, P., Kessler, D., Holtkötter, O., Shepard, P., Mauch, C. & Krieg, T. (2000) Fibroblast–matrix interactions in wound healing and fibrosis. *Matrix Biology* **19**, 325–332.

Fisher, L. W., Gehron Robey, P., Tuross, N., Otsuka, A. S., Tepen, D. A., Esch, F. S., Shimasaki, S. & Termine, J. D. (1987a) The 24,000 Mr phosphoprotein from developing bone is the *N*-propeptide of the alpha 1 chain of type I collagen. *The Journal of Biological Chemistry* **262**, 13457–13463.

Fisher, L. W., Hawkins, G. R., Tuross, N. & Termine, J. D. (1987b) Purification and partial characterization of small proteoglycans I and II, bone sialoproteins I and II, and osteonectin from the mineral compartment of developing human bone. *The Journal of Biological Chemistry* **262**, 9702–9708.

Fisher, L. W., Stubbs, J. T. I. & Young, M. F. (1995) Antisera and cDNA probes to human and certain animal model bone matrix noncollagenous proteins. *Acta Orthopaedica Scandinavica* **66** (Suppl. 266), 61–65.

Frank, R. M., Fiore-Donno, G., Cimasoni, G. & Matter, J. (1974) Ultrastructural study of epithelial and connective gingival reattachment in man. *Journal of Periodontology* **45**, 626–635.

Ganss, B., Kim, R. H. & Sodek, J. (1999) Bone sialoprotein. *Critical Reviews in Oral Biology and Medicine* **10**, 79–98.

Giannobile, W. V. & Somerman, M. J. (2003) Growth and amelogenin-like factors in periodontal wound healing. A systematic review. *Annals of Periodontology* **8**, 193–204.

Graziani, F., Laurell, L., Tonetti, M., Gottlow, J. & Berglundh, T. (2005) Periodontal wound healing following GTR therapy of dehiscence-type defects in the monkey. *Journal Clinical Periodontology* **32**, 905–914.

Grzesik, W. J. & Narayanan, A. S. (2002) Cementum and periodontal wound healing and regeneration. *Critical Reviews in Oral Biology and Medicine* **13**, 474–484.

Hammarström, L., Heijl, L. & Gestrelius, S. (1997) Periodontal regeneration in a buccal dehiscence model in monkeys after application of enamel matrix proteins. *Journal of Clinical Periodontology* **24**, 669–677.

Haney, J. M., Nilvéus, R. E., McMillan, P. J. & Wikesjö, U. M. E. (1993) Periodontal repair in dogs: expanded polytetrafluoroethylene barrier membranes support wound stabilization and enhance bone regeneration. *Journal of Periodontology* **64**, 883–890.

Herr, Y., Matsuura, M., Lin, W.-L., Genco, R. J. & Cho, M.-I. (1995) The origin of fibroblasts and their role in the early stages of horizontal furcation defect healing in the beagle dog. *Journal of Periodontology* **66**, 716–730.

Hsu, S. M., Raine, L. & Fanger, H. (1981) A comparative study of the PAP method and avidin biotin complex method for studying polypeptide hormones with radioimmunoassay antibodies. *American Journal of Clinical Pathology* **75**, 734–738.

Ivanovski, S., Li, H., Daley, T. & Bartold, P. M. (2000) An immunohistochemical study of matrix molecules associated with barrier membrane-mediated periodontal wound healing. *Journal of Periodontal Research* **35**, 115–126.

Jepsen, S., Eberhard, J., Herrera, D. & Needleman, I. G. (2002) A systematic review of guided tissue regeneration for periodontal furcation defects. What is the effect of guided tissue regeneration compared with surical debridement in the treatment of furcation defects? *Journal Clinical Periodontology* **29** (Suppl.), 103–116.

Kapila, Y. L., Lancero, H. & Johnson, P. W. (1998) The response of periodontal ligament cells to fibronectin. *Journal of Periodontology* **69**, 1008–1019.

Karring, T., Isidor, F., Nyman, S. & Lindhe, J. (1985) New attachment formation on the teeth with a reduced but healthy periodontal ligament. *Journal of Clinical Periodontology* **12**, 51–60.

Kawaguchi, H., Ogawa, T., Kurihara, H. & Nanci, A. (2001) Immunodetection of noncollagenous matrix proteins during periodontal tissue regeneration. *Journal of Periodontal Research* **36**, 205–213.

Kirkpatrick, P. & D'Ardenne, A. J. (1984) Effects of fixation and enzymatic digestion on the immunohistochemical demonstration of laminin and fibronectin in paraffin embedded tissue. *Journal of Clinical Pathology* **37**, 639–644.

Lao, M., Marino, V. & Bartold, P. M. (2006) Immunohistochemical study of bone sialoprotein and osteopontin in healthy and diseased root surfaces. *Journal of Periodontology* **77**, 1665–1673.

Larjava, H., Sandberg, M., Happonen, R.-P. & Vuorio, E. (1990) Differential localization of type I and type III procollagen messenger ribonucleic acids in inflamed periodontal and periapical connective tissues by in situ hybridization. *Laboratory Investigation* **62**, 96–103.

Laurell, L., Bose, M., Graziani, F., Tonetti, M. & Berglundh, T. (2006) The structure of periodontal tissues formed following guided tissue regeneration therapy of intra-bony defects in the monkey. *Journal Clinical Periodontology* **33**, 596–603.

Liu, H. W., Yacobi, R., Savion, N., Narayanan, A. S. & Pitaru, S. (1997) A collagenous cementum-derived attachment protein is a marker for progenitors of the mineralized tissue forming cell lineage of the periodontal ligament. *Journal of Bone and Mineral Research* **12**, 1691–1699.

MacNeil, R. L., Berry, J., D'Errico, J., Strayhorn, C., Piotrowski, B. & Somerman, M. J. (1995a) Role of two mineral-associated adhe-

© 2007 The Authors. Journal compilation © 2007 Blackwell Munksgaard

sion molecules, osteopontin and bone sialoprotein, during cementogenesis. *Connective Tissue Research* **33**, 1–7.

MacNeil, R. L., Berry, J., D'Errico, J., Strayhorn, C. & Somerman, J. (1995b) Localization and expression of osteopontin in mineralized and nonmineralized tissues of the periodontium. *Annals of the New York Academy of Sciences* **760**, 166–176.

MacNeil, L. M., Berry, J., Strayhorn, C. & Somerman, M. J. (1996) Expression of bone sialoprotein mRNA by cells lining the mouse tooth root during cementogenesis. *Archives of Oral Biology* **41**, 827–835.

MacNeil, R. L., D'Errico, J. A., Ouyang, H., Berry, J., Strayhorn, C. & Somerman, M. J. (1998) Isolation of murine cementoblasts: unique cells or uniquely-positioned osteoblasts? *European Journal of Oral Sciences* **106**, 350–356.

MacNeil, L. M., Sheng, N., Strayhorn, C. & Fisher, L. W. (1994) Bone sialoprotein is localized to the root surface during cementogenesis. *Journal of Bone and Mineral Research* **9**, 1597–1606.

MacNeil, L. M. & Somerman, M. J. (1999) Development and regeneration of the periodontium: parallels and contrasts. *Periodontology 2000* **19**, 8–20.

Matsuura, M., Herr, Y., Han, K.-Y., Lin, W.-L., Genco, R. J. & Cho, M.-I. (1995) Immunohistochemical expression of extracellular matrix components of normal and healing periodontal tissues in the beagle dog. *Journal of Periodontology* **66**, 579–593.

McCulloch, C. A. G. (1995) Origins and fuctions of cells essential for periodontal repair: the role of fibroblasts in tissue homeostasis. *Oral Diseases* **1**, 271–278.

McCulloch, C. A. G. & Bordin, S. (1991) Role of fibroblast subpopulations in periodontal physiology and pathology. *Journal of Periodontal Research* **26**, 144–154.

McKee, M. D. & Nanci, A. (1996a) Osteopontin at mineralized tissue interfaces in bone, teeth, and osseointegrated implants: ultrastructural distribution and implications for mineralized tissue formation, turnover, and repair. *Microscopy Research and Technique* **33**, 141–164.

McKee, M. D. & Nanci, A. (1996b) Secretion of osteopontin by macrophages and its accumulation at tissue surfaces during wound healing in mineralized tissues: a potential requirement for macrophage adhesion and phagocytosis. *The Anatomical Record* **245**, 394–409.

McKee, M. D., Zalzal, S. & Nanci, A. (1996) Extracellular matrix in tooth cementum and mantle dentin: localization of osteopontin and other noncollagenous proteins, plasma proteins, and glycoconjugates by electron microscopy. *The Anatomical Record* **245**, 293–312.

Melcher, A. H. (1976) On the repair potential of periodontal tissues. *Journal of Periodontology* **47**, 256–260.

Murphy, K. G. & Gunsolley, J. C. (2003) Guided tissue regeneration for the treatment of periodontal intrabony and furcation defects. A systematic review. *Annals of Periodontology* **8**, 266–302.

Nalbandian, J. & Frank, R. M. (1980) Electron microscopic study of the cementum and periodontal connective tissue attachment in the cat. *Journal of Periodontal Research* **15**, 71–89.

Nanci, A. (1999) Content and distribution of non-collagenous matrix proteins in bone and cementum: relationship to speed of formation and collagen packing density. *Journal of Structural Biology* **126**, 256–269.

Narayanan, A. S., Clagett, J. A. & Page, R. C. (1985) Effect of inflammation on the distribution of collagen types, I, III, IV, and V and type I trimer and fibronectin in human gingivae. *Journal of Dental Research* **64**, 1111–1116.

Needleman, I. G., Tucker, R., Giedrys-Leeper, E. & Worthington, H. (2002) A systematic review of guided tissue regeration for periodontal infrabony defects. *Journal of Periodontal Research* **37**, 380–388.

Nohutcu, R. M., McCauley, L. K., Koh, A. J. & Somerman, M. J. (1997) Expression of extracellular matrix proteins in human periodontal ligament cells during mineralization in vitro. *Journal of Periodontology* **68**, 320–327.

Ogata, Y., Niisato, N., Sakurai, T., Furuyama, S. & Sugiya, H. (1995) Comparison of the characteristics of human gingival fibroblasts and periodontal ligament cells. *Journal of Periodontology* **66**, 1025–1031.

Pontoriero, R., Nyman, S., Ericsson, I. & Lindhe, J. (1992) Guided tissue regeneration in surgically-produced furcation defects. An experimental study in the beagle dog. *Journal of Clinical Periodontology* **19**, 159–163.

Pritlove-Carson, S., Palmer, R. M., Morgan, P. R. & Floyd, P. D. (1992) Immunohistochemical analysis of cells attached to teflon membranes following guided tissue regeneration. *Journal of Periodontology* **63**, 969–973.

Reinholt, F. P., Hultenby, K., Oldberg, A. & Heinegard, D. (1990) Osteopontin – a possible anchor of osteoclasts to bone. *Proceeding of the National Academy of Science USA* **87**, 4473–4475.

Reynolds, J. J. & Meikle, M. C. (1997) Mechanisms of connective tissue matrix destruction in periodontitis. *Periodontology 2000* **14**, 144–157.

Romano, P. R., Caton, J. G. & Puzas, J. E. (1997) The reversal line may be a key modulator of osteoblast function: observations from an alveoar bone wound-healing model. *Journal of Periodontal Research* **32**, 143–147.

Saffar, J.-L., Lasfargues, J.-J. & Cherruau, M. (1997) Alveolar bone and the alveolar process: the socket that is never stable. *Periodontology 2000* **13**, 76–90.

Saygin, N. E., Giannobile, W. V. & Somerman, M. (2000) Molecular and cell biology of cementum. *Periodontology 2000* **24**, 73–98.

Schenk, R. K., Buser, D. & Dahlin, C. (1994) Healing pattern of bone regeneration in membrane-protected defects: a histological study in the canine mandible. *International Journal of Oral and Maxillofacial Implants* **9**, 13–29.

Schroeder, H. E. (1986) *The Periodontium*. Berlin: Springer.

Schroeder, H. E. (1992) Biological problems of regenerative cementogenesis: synthesis and attachment of collagenous matrices on growing and established root surfaces. *International Review of Cytology* **142**, 1–59.

Schwarz, F., Stratul, S.-I., Herten, M., Beck, B., Becker, J. & Sculean, A. (2006) Effect of an oily calcium hydroxide suspension (Osteoinductal) on healing of intrabony periodontal defects. A pilot study in dogs. *Clinical Oral Investigation* **10**, 29–34.

Sculean, A., Donos, N., Windisch, P., Brecx, M. C., Gera, I., Reich, E. & Karring, T. (1999) Healing of human intrabony defects following treatment with enamel matrix proteins or guided tissue regeneration. *Journal of Periodontal Research* **34**, 310–322.

Sculean, A., Junker, R., Donos, N., Berakdar, M., Brecx, M. & Dünker, N. (2002) Immunohistochemical evaluation of matrix molecules associated with wound healing following regenerative peiodontal treatment in monkeys. *Clinical Oral Investigations* **6**, 182.

Sculean, A., Junker, R., Donos, N., Windisch, P., Brecx, M. & Dünker, N. (2003) Immunohistochemical evaluation of matrix molecules associated with wound healing following treatment with an enamel matrix protein derivative in humans. *Clinical Oral Investigation* **7**, 167–174.

Sculean, A., Stavropoulos, A., Berakdar, M., Windisch, P., Karring, T. & Brecx, M. (2005) Formation of human cementum following different modalities of regenerative therapy. *Clinical Oral Investigations* **9**, 58–64.

Sigurdsson, T. J., Hardwick, R., Bogle, G. C. & Wikesjö, U. M. E. (1994) Periodontal repair in dogs: space provision by reinforced ePTFE membranes enhances bone and cementum regeneration in large supraalveolar defects. *Journal of Periodontology* **65**, 350–356.

Sodek, J., Ganss, B. & McKee, M. D. (2000) Osteopontin. *Critical Reviews in Oral Biology and Medicine* **11**, 279–303.

Somerman, M., Ouyang, H. J., Berry, J. E., Saygin, N. E., Strayhorn, C. L., D'Errico, J. A., Hullinger, T. & Giannobile, W. V. (1999) Evolution of periodontal regeneration: from the roots' point of view. *Journal of Periodontal Research* **34**, 420–424.

Somerman, M. J., Shroff, B., Agraves, W. S., Morrison, G., Craig, A. M., Denhardt, D. T., Foster, R. A. & Sauk, J. J. (1990) Expression of attachment proteins during cementogenesis. *Journal De Biologie Buccale* **18**, 207–214.

Stavropoulos, A. & Karring, T. (2005) Five-year results of guided tissue regeneration in combination with deproteinized bovine bone (Bio-Oss) in the treatment of intrabony periodontal defects: a case series report. *Clinical Oral Investigation* **9**, 271–277.

Stratul, S.-I., Schwarz, F., Becker, J., Willershausen, B. & Sculean, A. (2006) Healing of intrabony defects following treatment with an oily calcium hydroxide suspension (Osteoinductal). A controlled clinical study. *Clinical Oral Investigations* **10**, 55–60.

© 2007 The Authors. Journal compilation © 2007 Blackwell Munksgaard

Tonetti, M. S., Cortellini, P., Lang, N. P., Suvan, J. E., Adriaens, P., Dubravec, D., Fonzar, A., Fourmousis, I., Rasperini, G., Rossi, R., Silvestri, M., Topoll, H., Wallkamm, B. & Zybutz, M. (2004) Clinical outcomes following treatment of human intrabony defects with GTR/bone replacement material or access flap alone. A multicenter randomized controlled clinical trial. *Journal of Clinical Periodontology* **31**, 770–776.

Trombelli, L., Heitz-Mayfield, L., Needleman, I. G., Moles, D. & Scabbia, A. (2002) A systematic review of gaft materials and biological agents for periodontal intraosseous defects. *Journal Clinical Periodontology* **29** (Suppl.), 117–135.

van den Bos, T., Bronckers, A. L. J. J., Goldberg, H. A. & Beertsen, W. (1999) Blood circulation as a source of osteopontin in acellular extrinsic fiber cementum and other mineralizing tissue. *Journal of Dental Research* **78**, 1688–1695.

Werkmeister, J. A., Peters, D. E. & Ramshaw, J. A. (1989) Development of monoclonal antibodies to collagens for assessing host implant interactions. *Journal of Biomedical Materials Research* **23**, 273–283.

Werkmeister, J. A. & Ramshaw, J. A. (1988) The use of immunohistology in studies on connective tissue organization in hides and skins. *Das Leder* **39**, 145–151.

Werkmeister, J. A. & Ramshaw, J. A. (1989) Monoclonal antibodies to collagens for immunofluorescence examination of human skin. *Acta Dermatologica* **69**, 399–402.

Wikesjö, U. M. E. & Selvig, K. A. (1999) Peridontal wound healing and regeneration. *Periodontology 2000* **19**, 21–39.

Yamada, K. M., Akiyama, S. K., Hasegawa, T., Hasegawa, E., Humphries, M. J., Kennedy, D. W., Nagata, K., Urushihara, H., Olden, K. & Chen, W.-T. (1985) Recent advances in research on fibronectin and other cell attachment proteins. *Journal of Cell Biochemistry* **28**, 79–97.

Young, M. F., Kerr, J. M., Termine, J. D., Wewer, U. M., Wang, M. G., McBride, O. W. & Fisher, L. W. (1990) cDNA cloning, mRNA distribution and heterogeneity chromosomal location, and RFLP analysis of human osteopontin (OPN). *Genomics* **7**, 491–502.

Zappa, U. (1991) Resorbierbare membranen (II): Parodontale Geweberegeneration unter Verwendung von resorbierbaren Membranen – Histologische Aspekte. *Schweizer Monatsschrift für Zahnmedizin* **101**, 1321–1324.

Zeichner-David, M. (2006) Regeneration of periodontal tissues: cementogenesis revisited. *Periodontology 2000* **41**, 196–217.

Address:
Michael Christgau
Luegplatz 3
40545 Düsseldorf
Germany
E-mail: michael.christgau@klinik.uni-regensburg.de

Clinical Relevance

Scientific rationale for the study: The high variability and low predictability of periodontal regeneration therapy requires a better understanding of essential cellular and molecular mechanisms necessary for the regeneration process.

Principal findings: This immunohistochemical investigation revealed in general a similar temporal and spatial expression pattern of important ECM proteins following regenerative and conventional periodontal therapy, although the quality of wound stabilization and inflammatory reactions had a significant influence on the timing and quantity of ECM expression.

Practical implications: A future therapeutic strategy might deliver key ECM proteins to attract the relevant cells for periodontal regeneration.

© 2007 The Authors. Journal compilation © 2007 Blackwell Munksgaard

This document is a scanned copy of a printed document. No warranty is given about the accuracy of the copy. Users should refer to the original published version of the material.